61,684
File Copy

TEMPERATURE LOGS IN PRODUCTION AND INJECTION WELLS

by J. LOEB and A. POUPON

S.P.E. SCHLUMBERGER - PARIS

Nice, Quantitative Description

PAPER PRESENTED AT THE TWENTY-SEVENTH MEETING OF THE EUROPEAN ASSOCIATION OF EXPLORATION GEOPHYSICISTS IN MADRID - MAY 5-6-7-1965

B.3.1.2.3.1

TEMPERATURE LOGS IN PRODUCTION AND INJECTION WELLS

by J. Loeb and A. Poupon

INTRODUCTION

Both in production wells and in injection wells reliable quantitative information about fluid movements can be obtained with the Production Logging tools :

- Packer Flowmeter, to measure flow rates not exceeding about 2,000 barrels per day at bottom hole conditions ; in the future the Packer Flowmeter will be equipped with fluid analyzing devices, to determine the approximate proportions of oil, gas and water in the flow.
- Continuous Flowmeter, for flow rates higher than about 1,000 barrels per day.
- Gradiomanometer, to measure the pressure gradient, from which the average density of the fluids in the well can be derived.
- Caliper to measure hole diameters in the case of barefoot completions.
- Cement Bond Tool, to evaluate the quality of the cementation.
- Neutron Log, responding to the presence of gas in the formations and in the casing.
- High Resolution Thermometer.

All these tools have small diameters and can be lowered through tubing against well head pressures of as much as 4,000 psi without any interruption of the production or injection.

The Thermometer is of great interest, because the temperature profiles will pin-point gas entries, usually shown by a substantial cooling effect due to gas expansion, and will also - and this is even more important - give information about possible fluid movements behind pipe (casing, liner, or tubing).

There have been already several publications about temperature logs in production and injection wells (see references) but in these the case of vertical communication behind pipe is not considered. Besides in the case of gas wells, the effect of the expansion of the gas as it flows upwards is not taken into account ; consequently actual temperature profiles in gas wells do not always have the shape predicted in these earlier publications.

THEORETICAL CONSIDERATIONS AND DERIVATIONS

- Mechanism of heat exchange -

It is assumed that at the time when the temperatures are measured, production, or injection, is under well stabilized conditions, and that the temperature remains constant at any given point in the system considered (fluids, casing, formations).

Heat exchange between the moving fluid and the casing is through forced convection in relation with the fact that temperature equilibrium cannot be attained since the fluid in contact with the casing is continuously renewed. In the case of a stagnant fluid heat exchange is through natural convection.

The parameters involved are :		(units : M K S system) *Kilogram always designates the unit of mass*
A	inside cross section of the casing	square meters
D	inside diameter of the casing	meters
V	velocity of the fluid	meters/second
v_s	specific volume of the fluid	cubic meters per kilogram
ρ	density of the fluid	kilograms per cubic meter
C_p	specific heat of the fluid at constant pressure	kilocalories per kilogram per ° C
μ	viscosity of the fluid	kilograms second per square meter
λ	thermal conductivity of the fluid	kilocalories per meter per hour per ° C
k	thermal conductivity of the formation	kilocalories per meter per hour per ° C
g	acceleration of gravity	9.8 meters per second per second
T	temperature	degrees Centigrade
α	coefficient of heat exchange	kilocalories per square meter per hour per ° C
p	pressure	Pascal
G	geothermal gradient, vertical distance over which the temperature of the formations varies by 1° centigrade	meters

The quantity of heat q (in kilocalories per square meter per second) flowing across the casing is proportional to the difference between the temperature T of the fluid and the temperature T_c of the casing :

$$q = \alpha (T - Tc)$$

The quantity α is derived from the following dimensionless numbers :

the Reynolds number $$R = \frac{\rho V D}{\mu g}$$

the Prandtl number $P = \frac{C_p \mu g}{\lambda / 3600}$

the Biot (or Nusselt) number $B = \frac{\alpha D}{\lambda}$

α is given by empirical relationships :

for liquids 1) $B = .0225\ R^{.8}\ P^{.4}$

for gases 1') $B = .02 R^{.8}$

Typical values of α range from a few hundred to a few thousand kilocalories per square meter per hour per degree centigrade.

Heat exchange between the casing and the formation is through thermal conductivity, without any discontinuity of the temperatures.

It is assumed that there is no vertical heat transfer other than that due to vertical fluid movement.

- Enthalpic Balance -

Let z be the distance measured upward along the axis of the casing from some convenient reference point. Considering a small interval between z and $z + \Delta z$, since the temperature does not change with time, the quantity of energy corresponding to the variation of the temperature T of the fluid with depth compensates the losses of heat across the casing, the expansion of the fluid (for gases) and the action of gravity.

For liquids :

2) $\Delta Q = - A \rho V C_p \frac{dT}{dz} \Delta z$

For gases :

3) $\Delta Q = - A \rho V \left(C_p \frac{dT}{dz} - v_s \frac{dp}{dz}\right) \Delta z$

The action of gravity results in :

4) $\frac{dp}{dz} = - \frac{g}{v_s}$

this, carried into 3), gives

5) $\Delta Q = - A \rho V C_p \left(\frac{dT}{dz} + \frac{1}{y}\right) \Delta z$

where $y = \frac{C_p}{g}$ is a length.

Finally, between the casing and the formations heat exchange is defined by a Neumann problem: knowing T and Tc, the heat flux across the casing is known ; in addition the temperature of the formations Te (z) at a sufficient distance from the well is known. It is assumed here that :

6) $Te(z) = To - 1^\circ C \times \frac{z}{G}$

In the case of gas production, (methane), for V = 2 m/sec (at a depth of 8,000 feet this would correspond to a daily production of the order of 30.000.000 cubic feet measured at surface conditions), we find :

$$\frac{J\,(1+\beta)}{\beta} = 1800 \text{ meters}$$

and $$\frac{J\,(1+\beta)}{\gamma\,\beta} = 17^{\circ} \text{ Centigrade}$$

- Practical application of differential equations 8) and 9) -

In fact, these are not linear differential equations, as the coefficients C_p ρ and α depend on temperature. It would be possible, through the use of electronic computers, to obtain accurate solutions. However, this is not necessary, as the need is mainly for predicting the shapes of the temperature profiles, particularly at levels where fluid is produced - or absorbed - by a formation. Since, in addition, the intervals of interest are often fairly short, with temperature variations not exceeding 10 or possibly 20° Centigrade, it is sufficient to consider the solution for constant values of the coefficients corresponding to the usual practical range of temperatures and pressures. With these limitations then, equations 8) and 9) indicate that the temperature profile, for a constant flow rate, is an exponential curve with an asymptote parallel to the geothermal profile. In the case of liquids, this asymptote is shifted horizontally (temperatures being plotted in abscissae, depths in ordinates) with respect to the geothermal profile by a quantity.

$$1^{\circ} \text{ Centigrade} \times \frac{L\,(1+\beta)}{G\,\beta}$$

towards higher temperatures in the case of production, towards lower temperatures in the case of injection. For the numerical example considered hereabove, and for G = 33 meters, this shift ΔT would be :

$$1^{\circ} \text{ Centigrade} \times \frac{L\,(1+\beta)}{G\,\beta} = 1840/33 = 56^{\circ} \text{ Centigrade}$$

For the gas producing well the shift ΔT would be :

$$1^{\circ} \text{ Centigrade} \times \frac{J\,(1+\beta)}{\beta}\left[\frac{1}{G} - \frac{1}{\gamma}\right] = 38^{\circ} \text{ C}$$

Computations made for the case of a cylindrical pipe of infinite length lead to a solution where the temperature varies as a logarithmic function of the radial distance to the axis of the well ; this is not compatible with the condition that at a sufficient distance T (r, z) be equal to Te (z).

On the contrary computations can be made without any difficulty for the case of an elongated ellipsoid of revolution and it is found that at the equator of the ellipsoid :

7) $\frac{2k}{D\alpha} \quad (T_c - T_e) = T - T_c$

the quantity $\frac{2k}{D\alpha} = \beta$ is a dimensionless number.

Case of liquids

Combining 2) and 7), it is found that :

8) $L \frac{(1+\beta)}{\beta} \frac{dT}{dz} + T = T_e \ (z)$

Where $L = \frac{A}{\pi D} \times \frac{PR}{B}$ is a length

Case of Gases

It is found that

9) $J \frac{(1+\beta)}{\beta} \frac{dT}{dz} + T = T_e \ (z) - \frac{J \ (1+\beta)}{\gamma \beta}$

Where $J = \frac{A}{\pi D} \times \frac{C_p \rho V}{\alpha}$ is a length

Equation 9) is very similar to 8) ; for a given flow rate the term $\frac{J \ (1+\beta)}{\gamma\beta}$ is constant ; this shows that in the case of gas production, due to the cooling effect in relation with the expansion of the gas, the temperature profile is the same as would be observed for a non compressible fluid but with formation temperatures which would be lower by a fixed amount

$$1^\circ \ C \times \frac{J \ (1+\beta)}{\gamma \beta}$$

Numerical examples

Let $D = .20$ m $\qquad \frac{A}{\pi D} = .05$ m

In case of oil production, for V = .10 m/second (approximately 1700 barrels per day), we find

$$L \ (\frac{1+\beta}{\beta}) \doteq 1840 \text{ meters}$$

RESULTS

Using the results of the theoretical study, temperature profiles have been determined for a number of typical cases, so as to provide a sound basis for the interpretation of actual temperature logs. In all cases considered hereafter it is assumed that the producing intervals (or the intervals taking fluid) are very thin ; it is also assumed that the geothermal profile is a straight line (T T' on all the figures).

- A : Oil Production -

A - 1

One interval P is producing ; there is no vertical movement behind the casing, so that the oil entering the casing is at the temperature given by the geothermal profile at the corresponding depth. Starting from bottom, the temperature curve follows the geothermal profile up to the point of oil entry. Above this point, the curve is an exponential, with an asymptote A A' parallel to the geothermal line : the horizontal distance ΔT between the geothermal line and the asymptote can be expressed as a function of the mass flow rate M and of the casing diameter D :

$$\Delta T = \frac{1}{G} (a M^{.2} D^{.8} + b M)$$

a and b are coefficients depending essentially on the physical characteristics of the fluid produced, and the thermal conductivity of the formations.

In practice the relative values of coefficients a and b are such that the first term in the above expression of ΔT is negligible as compared to the second one, and accordingly ΔT is practically proportional to the weight of fluid produced per unit time ; the size of the casing has very little effect. The shape of the curve, and the construction of the tangent at any point E are shown on figure A 1 : draw E N horizontally, then N O vertically, O E is the tangent at E. At P the tangent is vertical.

A - 2

Two intervals, P_1 and P_2, are producing, with production rates M_1 and M_2. From bottom to P_2 the temperature curve has the shape indicated on figure A - 1. At P_2 there is an abrupt decrease of temperature. The oil from P_1 being at temperature T_1, the oil from P_2 at T_2 (geothermal profile), the mixture of the two takes the temperature T given by :

$$(M_1 + M_2)\ T = M_1\ T_1 + M_2\ T_2$$

The increased flow, above P_2, causes a displacement toward the right of the asymptote (see figure A-2) ; the position of this second asymptote $A_2\ A'_2$ with respect to the geothermal profile is given by :

$$\Delta T \cong \frac{b}{G} (M_1 + M_2)$$

A - 3

At depth S, all the flow enters a tubing ; above S temperature exchange between the flowing fluid and the formations is through natural convection of the oil which is trapped in the annular space between tubing and casing ; the temperature curve remains exponential in shape, but as the coefficient of the natural convection is considerably smaller than that corresponding to the forced convection, the asymptote $A_2 A'_2$ is much further to the right (figure A - 3).

A - 4

The flow is through the annular space between tubing and casing ; the fluid in the tubing does not move : in this case, the temperature observed in the tubing will be practically the same as if there were no tubing ; hence at the level of the tubing shoe the curve will show no significant change.

A - 5

The flow is through the annular space, and some fluid is lost at depth F. The fluid loss causes a shift toward the left of the asymptote, hence the point of fluid loss will be shown by a change of slope on the temperature curve, fig. A 5-1 and A 5-2. Figure A 5-3 is for the case where no fluid is produced at the surface.

A - 6

Oil flows upward from P_1 , between casing and formations, and enters the casing at P_2 : the temperature curve is practically the same as if the oil entered the casing at P_1 . In this case the temperature profile shows the origin P_1 of the oil, whereas a flowmeter will indicate the point of entry in the casing P_2.

A - 7

Oil flows downward from P, between the casing and formations and enters the casing at P'. Below P' the curve follows the geothermal profile ; at P' there is an abrupt temperature decrease ; then the variation of temperature with depth follows a curve which has a vertical tangent at the level of P'. At P there is a change of slope. Above P the curve is as in case A-1 (Figure A-7).

A - 8

As for A - 7 there is a downward flow behind casing from P to P', but there is also oil production at P'. The curve is similar to that of case A - 7, however the temperature anomaly at P' is smaller and the tangent at P' is no longer vertical (figure A - 8).

A - 9

There is no production ; oil flows downward from P into P', either inside the casing, or behind the casing ; due to the downward flow, the asymptote is to the left (side of lower temperatures) of the geothermal profile (figure A - 9).

- B : Gas Production -

The gas expands as it escapes from the reservoir rock into the casing ; this causes a substantial cooling, and accordingly the gas when it enters the casing is at a lower temperature than the formation from which it comes. Besides, the gas as it moves upward continues to expand and this expansion absorbs heat. As in the case of oil production, the temperature profile is an exponential curve, but the cooling due to gas expansion causes a shift toward the lower temperatures of both the asymptote and the parallel straight line from which the tangents to the temperature profile can be constructed (this « guide-line » is the geothermal profile in the case of oil production). The horizontal distance ΔT between the « guide-line » and the asymptote is still given by.

$$\Delta T \equiv - \frac{b M}{G}$$

as in the case of oil ; however, gas and oil having different specific heats, the corresponding coefficients are also different. The horizontal distance by which the « guide-line » and the asymptote are shifted toward the lower temperatures is given by $\frac{b M g}{C_p}$ where g is the acceleration of gravity (9.8 m/sec/sec) and C_p the specific heat of the gas at constant pressure ; this is proportional to ΔT and would be equal to about one third of ΔT in the case of methane. Four cases only will be considered :

B - 1

One interval P is producing ; there is no vertical movement behind the casing. The positions of the « guide-line » and of the asymptote depend on the production rate, as seen here above. Two cases are possible : if the permeabilities are comparatively low, there is a fairly large pressure drop between the reservoir and the casing, and the gas when it enters the casing is at a temperature lower than that corresponding to the « guide-line » : then the gas will first be heated up by the formations ; the tangent will be vertical where the curve crosses the « guide-line » and above this point the gas becomes colder due to the combined effects of heat exchange with the formations and gas expansion. If the permeabilities are relatively high, the pressure drop between reservoir and casing is small and the gas when it enters the casing is at a temperature higher than that corresponding to the « guide-line » ; in this case there is no warming up of the gas, and no reversal of the slope of the temperature profile. The two cases are shown on figure B - 1.

B - 2

Two intervals P_1 and P_2 are producing. To flow rates M_1 and $M_1 + M_2$ correspond two sets of guide lines and asymptotes $L_1\ L'_1$, $A_1\ A'_1$ and $L_2\ L'_2$, $A_2\ A'_2$ (figure B - 2).

B - 3

Gas escapes from the formation at P, moves upward behind the casing and enters the casing at P'. There is a cooling effect due to gas expansion at P, and probably also at P' ; both parts of the temperature curve, between P and P', and above P, have the same guide line and the same asymptote (figure B - 3).

B - 4

Gas escapes from the formation at P, moves downward behind the casing and enters the casing at P'. In this case again there is gas expansion at P and at P' but the temperature log shows an abrupt temperature variation only at P' ; at P there is a change of slope, as shown on figure B-4.

- C : Water Injection -

The temperature profiles are again exponential curves. As the water flows downward the asymptote AA' is on the low temperature side of the geothermal line, at a horizontal distance ΔT given by $\Delta T = - \frac{b M}{G}$

C - 1

One interval takes fluid. The shape of the curve, and the construction of the tangents are shown on figure C-1. Where the curve crosses the geothermal line, the tangent is vertical.

C - 2 and C - 3

Two intervals P_1 and P_2 take fluid, at mass flow rates M_1 and M_2 .

Above P_1 the position of asymptote $A_1 A'_1$ corresponds to total flow rate $M_1 + M_2$, whereas below P_1 asymptote $A_2 A'_2$ is determined by flow rate M_2. At the level of P_1, there is a change of slope on the temperature curve. Cases C_2 and C_3 are similar ; however in case C-3 there is a reversal of the curvature at P_1, because the curve overshoots asymptote $A_2 A'_2$ (case C-3 is similar to case A 5-1, while C-2 is similar to A 5-2).

- D : Gas Injection

As the gas flows downward, its pressure increases ; the compression produces heat. As a result the guide-line and the asymptote are shifted to the right, that is toward higher temperatures, by an amount proportional to the mass flow rate, and equal to about one third of $\Delta T = - \frac{b M}{G}$.

As in the case of gas production, a variation of the flow rate will produce a corresponding horizontal displacement of both the asymptote and the guide-line. Cases D_1 D_2 D_3 are very similar to cases C_1 C_2 C_3 .

FIELD EXAMPLES

Example 1

This is an unusual case : nevertheless, this temperature profile is thought to be of great interest, as it is a striking illustration of the ability of temperature logs to give information about fluid movements behind pipe.

In this well a 7" casing was run down to 1300 meters. Some 20 hours after the cementation, the well started blowing oil and gas from the annular space between the surface pipe and the 7" casing. A temperature log was recorded a few days later in the 7" casing. From the bottom to 825 m, the curve is practically a straight line and the temperatures probably do not depart significantly from the geothermal profile, indicating that there is no fluid movement below 825 m. Between about 825 m and 660 m the temperature curve presents several anomalies in relation with the blow out ; at 820 m the production is probably oil ; at 750 m the large cold anomaly clearly indicates gas production ; there is also gas production at about 725 m and 675 m. There is production also at 785 m but it is not too certain whether it is oil (probably), or gas. The very smooth shape of the curve indicates that the formations above 650 m were not producing.

The hydrocarbon bearing permeable formations, as determined from the open-hole electric logs, are shown on the figure ; there are other hydrocarbon bearing permeable formations, below 1100 m.

After this temperature survey, perforations were made at 800 meters and the upper part of the 7" casing was successfully cemented.

Example 2

At the time of the survey this well was producing 1660 barrels per day of oil with a Gas Oil Ratio of 1050 (the solution GOR was about 400) and a water cut of 14%.

The reservoir is a 150 foot limestone and dolomite, the structure is very flat. There is a gas-cap and the gas-oil contact is at a fairly short vertical distance - less than 100 feet - above the upper perforations, but the well is at a large horizontal distance from the edge of the gas cap.

Two intervals, A and B, are perforated. According to the Flowmeter and Gradiomanometer logs, interval A contributes very little to the total production. The Gradiomanometer indicates a large gas entry opposite the lower half of interval B.

The temperature log recorded in the flowing well gives large cold anomalies not only opposite interval B but also near the bottom of interval A ; the only possible explanation seems to be that a sizeable quantity of gas was being produced at that depth ; for some reason, this gas was not entering the casing through perforations A, but through perforations B.

That this was possible was confirmed by a cement bond log (Through Tubing CBT-B tool) which indicated a very poor bond between A and B ; it also indicated a very good bond below interval A.

The information given by the logs about the origin, or the point (s) of entry of the water produced, is not as clear. However the two temperature logs, made during production and with the well shut-in, show no significant departure below interval A from the expected geothermal profile other than a normal downward spreading of the cold anomaly due to the lower gas entry ; accordingly, it seems that no water was channeling up behind casing from below interval A ; this is confirmed by the good bond indication given by the CBT-B log (not shown).

The temperature log in the producing well covered an interval of only 100' above B and, as a consequence, it does not seem possible to reach a definite conclusion about the possibility of the water coming from higher up.

Example 3

This example correspond to a water injection well. The well has a 5 1/2" casing, perforated for water injection at 3,220-3,270.

The first temperature survey (dashed curve) was recorded after the well had been shut-in several hours. Then injection was resumed, at a rate of about 800 barrels per day, and another temperature survey (solid curve) was made after 20 hours. The approximate geothermal profile is also shown on the figure.

Looking at the temperatures recorded during injection, we see that the water is injected at a temperature in excess of 110° F. The water being at a much higher temperature than the formations near surface, the formations cool down the water. At about 1,200 feet the water (solid curve) and the formations (geothermal profile) are at the same temperature. Then below 1,200', the formations, being at a higher temperature, warm up the water. At about 3,270' there is an abrupt temperature increase and the temperature measured at the bottom of the well is approximately that of the geothermal profile. This confirms that no water is flowing downward past 3,270'.

Looking now at the dashed curve, we see that when injection stops, the temperatures in the fluid column change rapidly and tend to become equal to the temperature of the formations (geothermal profile). There is a striking exception, however ; opposite the perforations, in spite of the fact that the temperature recorded is some 22° F lower than the temperature of the geothermal profile, the change is much smaller. At that depth it would take many days to establish temperature equilibrium, and reach a temperature equal to that of the geothermal profile.

This can be explained as follows. At 3,000', for example, the water flowing downward being colder than the formations cools down the formations, but only to a short distance from the casing because the thermal conductivity of the formations is low ; when injection is stopped the formations rapidly warm up the water in the casing. At the level of the perforations, the water flows into the formations and lowers the temperature of the formations to a considerable distance (depending not on thermal conductivity, this time, but mostly on flow rate and porosity) ; accordingly a long time is needed to warm up to equilibrium temperature the formations and the fluid in casing. Of course, near the bottom, where the temperatures have never been disturbed by the injection, there is no significant temperature difference between the solid and the dashed curves.

The two temperature curves then clearly show that the water was going into the formations at 3220-3270, as expected, yet a continuous flowmeter indicated that the casing was leaking at about 600', and that no water was flowing downward inside the casing below that depth. This means then that, in spite of the casing failure, the water was reaching the right formations, flowing downward behind the casing below 600'.

It seems that all the water leaving the casing at about 600' was reaching the formations at 3220'-3270' . Any other formation taking water would have been indicated by an appreciable change of the slope of the temperature profile, and also by a much slower rate of variation of temperature after injection is stopped, as observed at 3220-3270.

As expected from the theoretical study, the temperature log does not show any significant anomaly at the depth of the casing leak.

Example 4

This corresponds to another water injection well in the same field. The 5 1/2" casing has several perforated intervals between 3260' and 3300'.

The solid curve was recorded during injection, with an injection rate of about 800 barrels per day. Then the injection was stopped and, after 13 hours, the dashed curve was recorded. The approximate geothermal profile is also shown.

Below about 1400' the dashed curve and the solid curve are identical and remain very close to the expected geothermal profile and both curves have a fairly constant slope about equal to that of the expected geothermal profile. These three features indicate that no water at all had reached that depth of about 1400'. A continuous flowmeter, made a few days later, showed that all of the injected water was leaving the casing at 180'.

Where was the water going ? Above about 330' the temperature changes rapidly when injection stops ; this, as already explained, indicates that the temperature disturbance affects only a small volume of formations close to the casing ; the formations above 330' probably were not taking water.

The abrupt change of slope at about 1,200-1,250' of the temperature curve recorded during injection may well correspond to the lowest formations taking water ; between 800' and 1,250', the two temperature curves do not differ much but, as already explained, the temperatures are expected to change slowly opposite formations taking water.

The water, then, is probably going into formations located between about 400' and 1250'. It does not seem possible to carry the interpretation further without some additional information : depths of permeable formations (these would be given by the open hole electrical logs) and geothermal profile.

The fact that the temperature profile recorded during injection does not look quite as would be expected from the theoretical considerations has several possible explanations :

- the temperature of the water injected probably is not constant
- there is a second string of casing, of larger diameter, down to about 800' ; thus it would be possible for example to have a downward flow in the annular space between the two casings and an upward flow behind the larger casing.

In any case, the Temperature log very clearly shows that the water does not reach the right formation and that it goes somewhere between about 400' and 1250' .

CONCLUSIONS

The theoretical curves of figures A, B, C and D show what kind of information temperature logs can be expected to give in production wells and in injection wells ; with the help of the other production logs, as explained for example in case A-6, it should be possible to detect vertical fluid movements of any significance behind pipe. The theoretical derivations are very well confirmed by the actual temperature profiles. Besides both the theoretical figures (A 5-3 for example) and the actual logs show that better information is obtained if the temperature logs are recorded not only during stabilized production or injection, but also after a shut-in period of several hours.

ACKNOWLEDGEMENTS

The courtesy of the Oil Companies who released the logs and corresponding data is gratefully acknowledged.

REFERENCES

Nowak T.J. 1952 : « *The Estimation of Water Injection Profiles from Temperature Surveys* » Petroleum Transactions of the AIME, Vol. 198, 1953

Bird J.M. 1954 : « Interpretation of Temperature logs in Water and Gas system Wells and Gas Producing Wells » Producers Monthly August 1954.

Kunz K.S. and Tixier M.P.T. 1955 : « Temperature Surveys in Gas Producing Wells » Journal of Petroleum Technology, July 1955

Schonblom J.E. 1961 : « Quantitative Interpretation of Temperature Logs in Flowing Gas Wells » Annual Meeting of the Society of Professional Well Log Analysts, May 1961

Loeb J. 1965 : « Sur l'Interpretation des Mesures Thermométriques », manuscript February 1965.

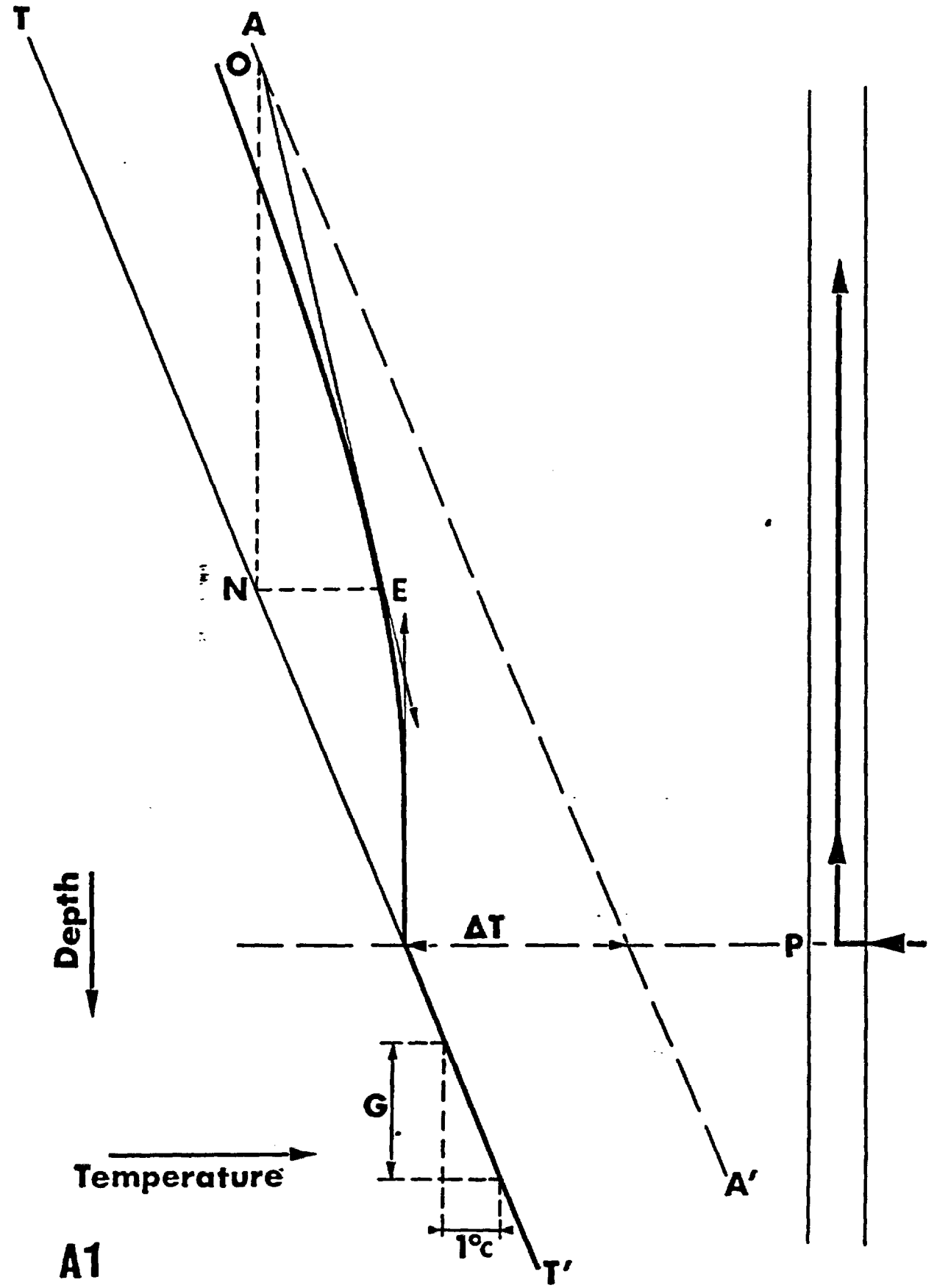

A1

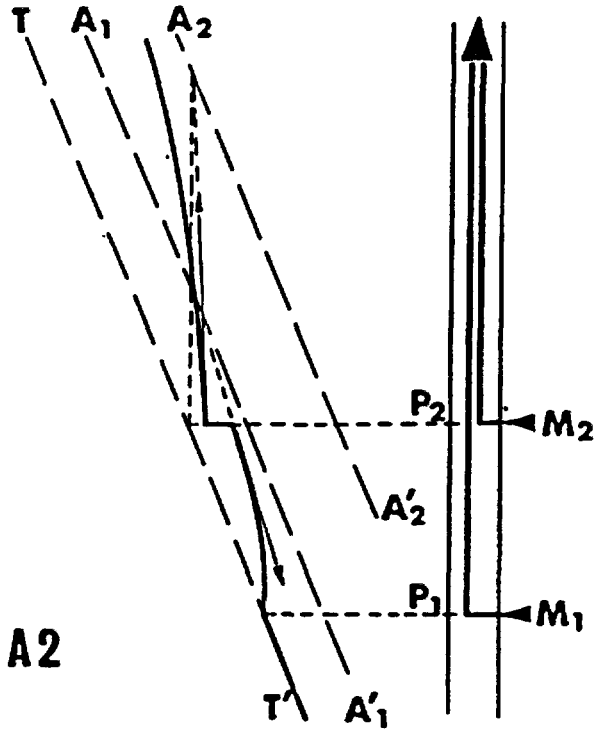

A2

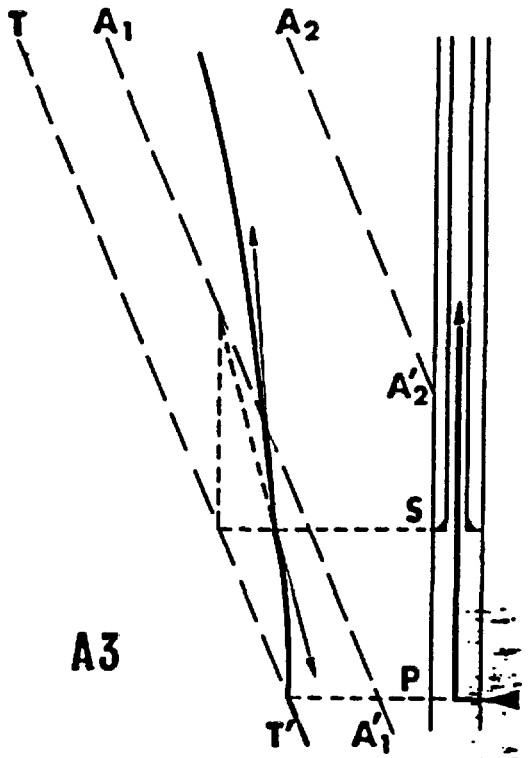

A3

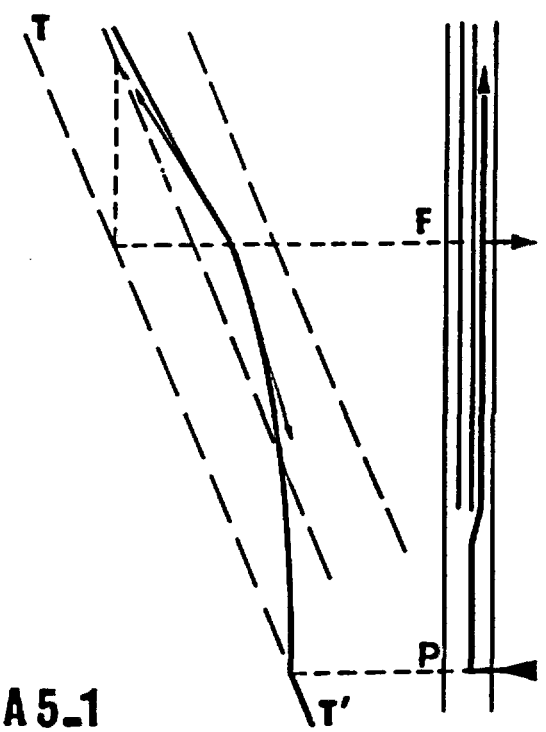

A5_1

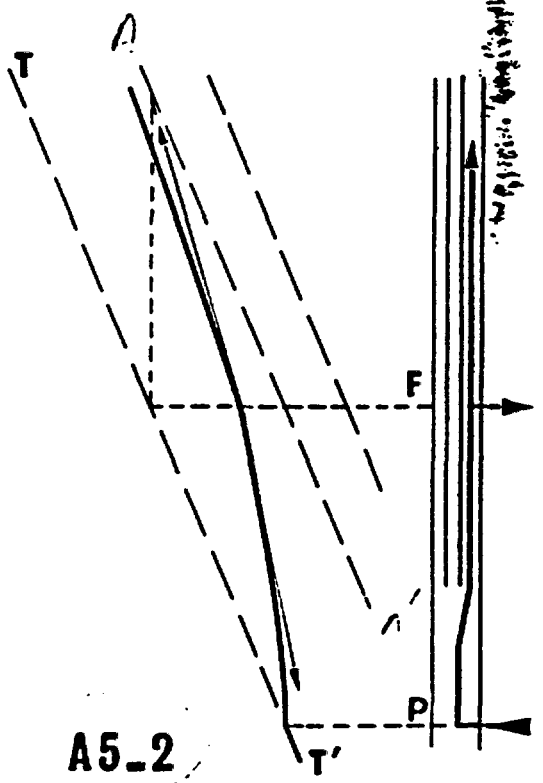

A5_2

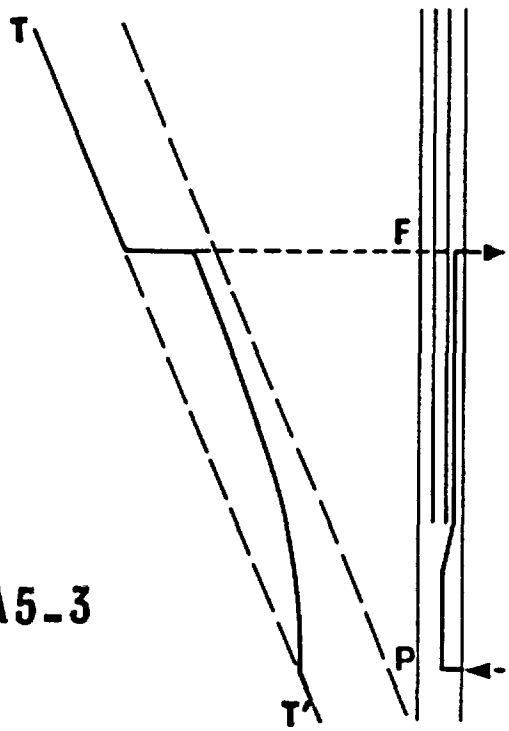

A5-3

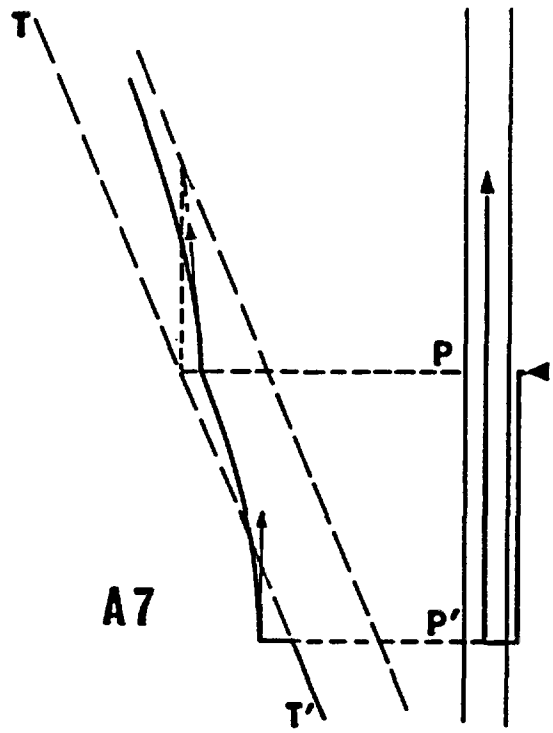

A7

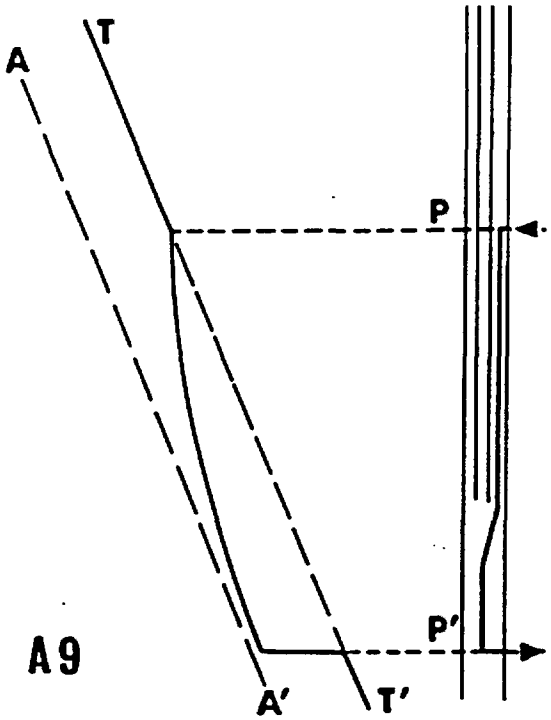

A9

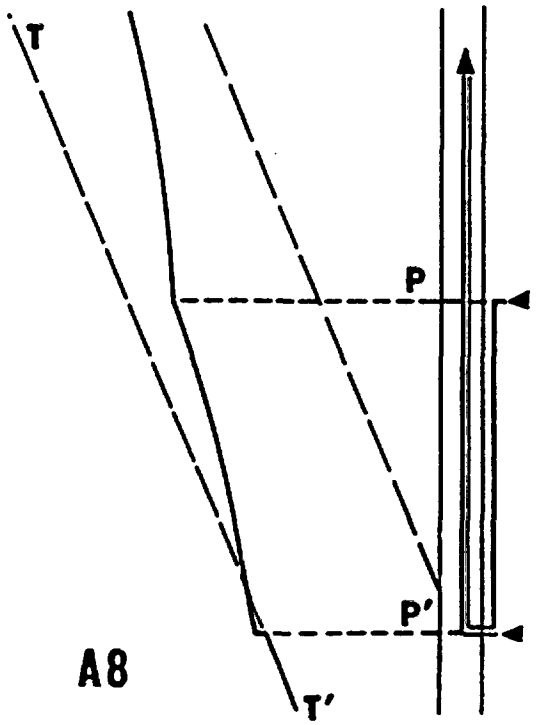

A8

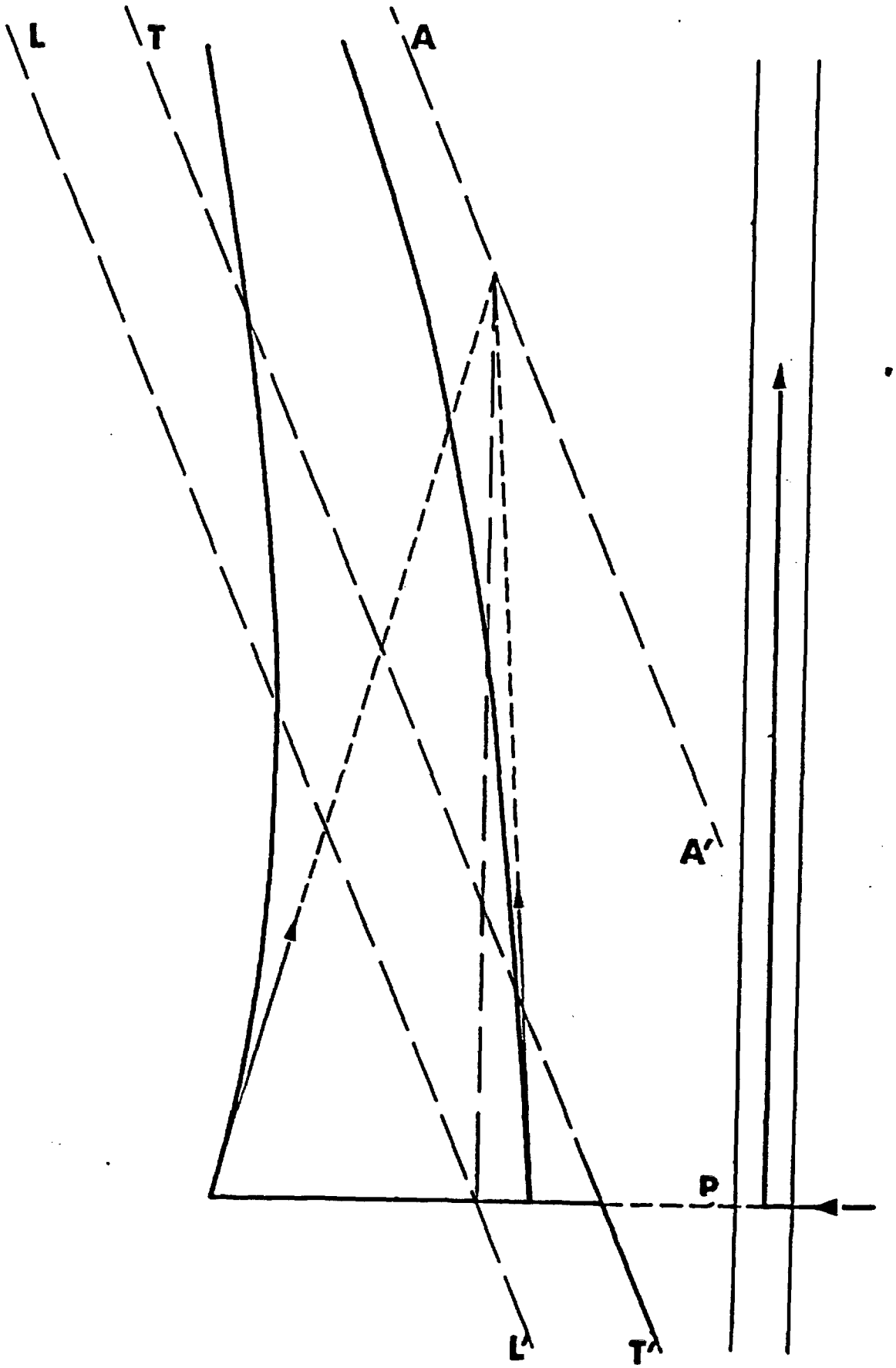

B1

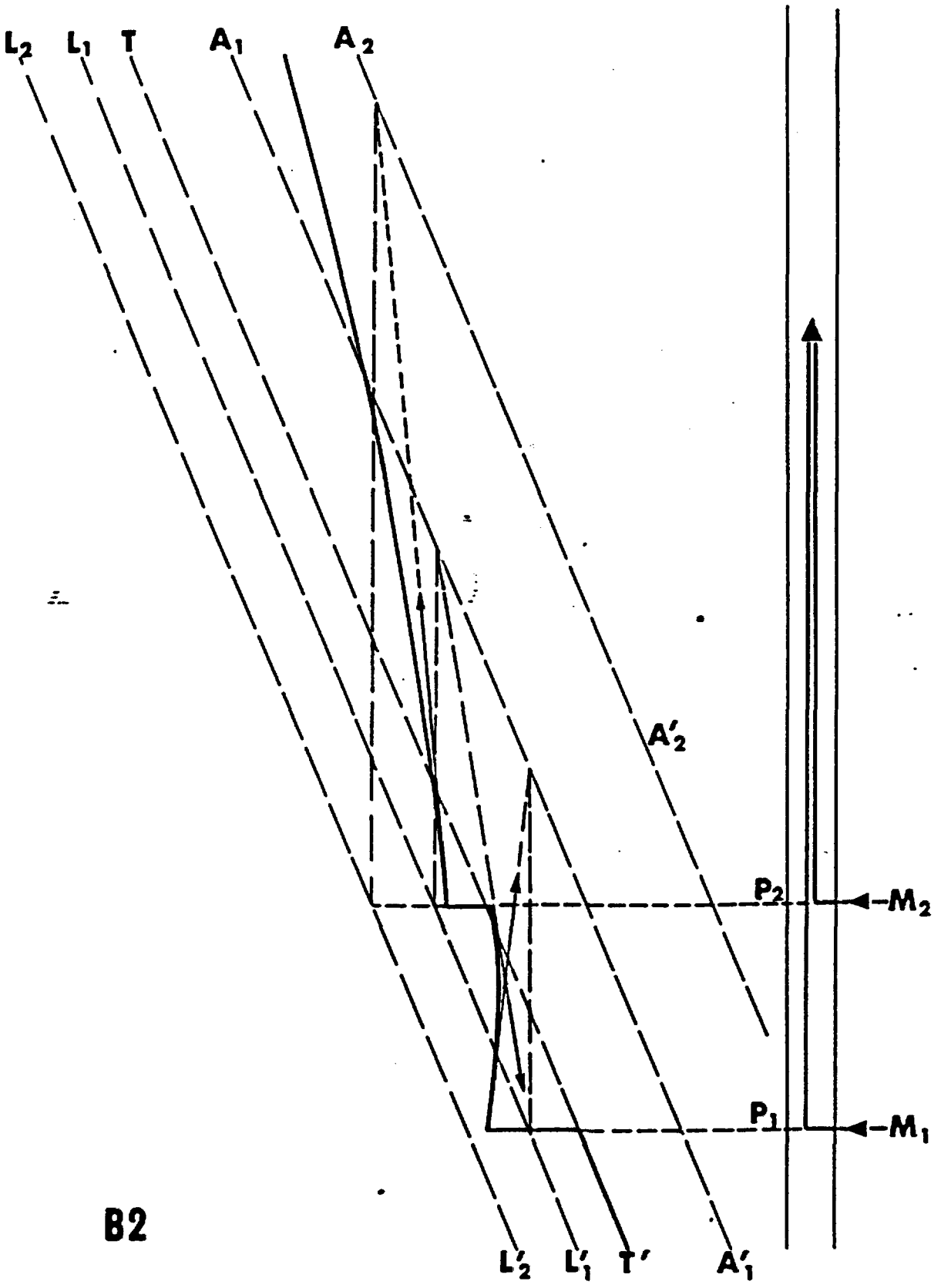

B2

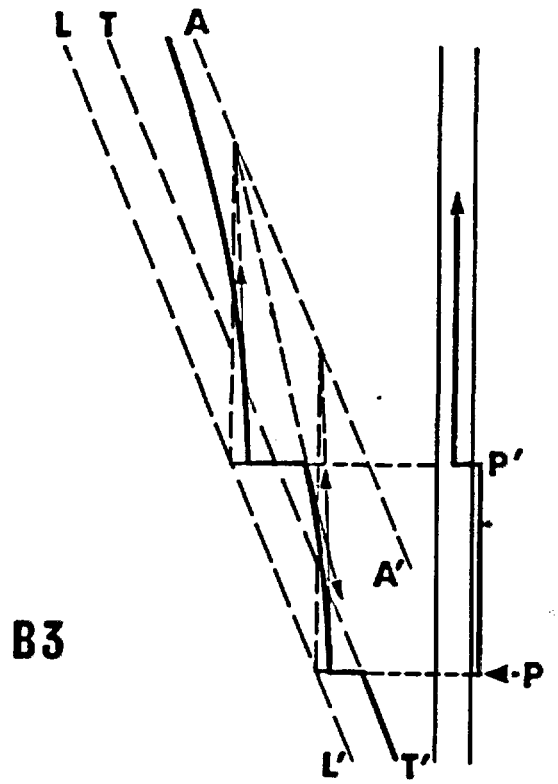

B3

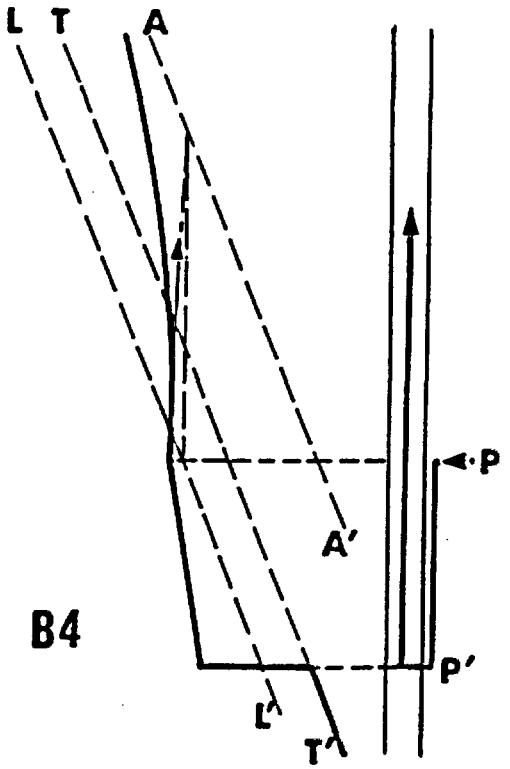

B4

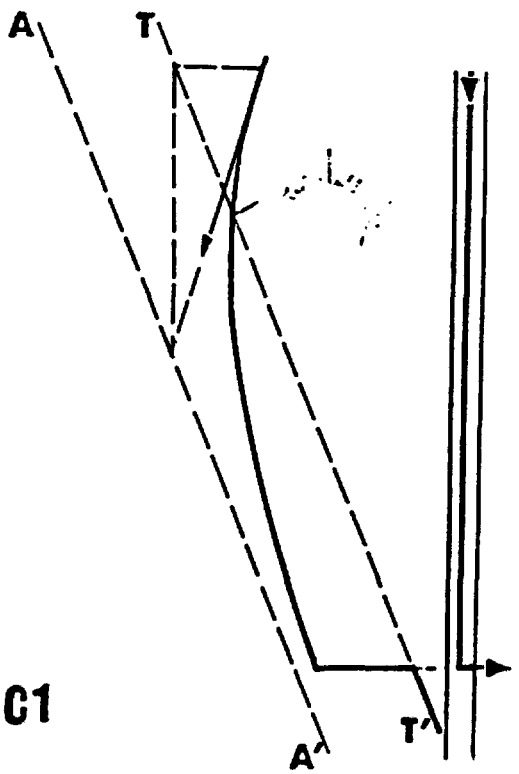

C1

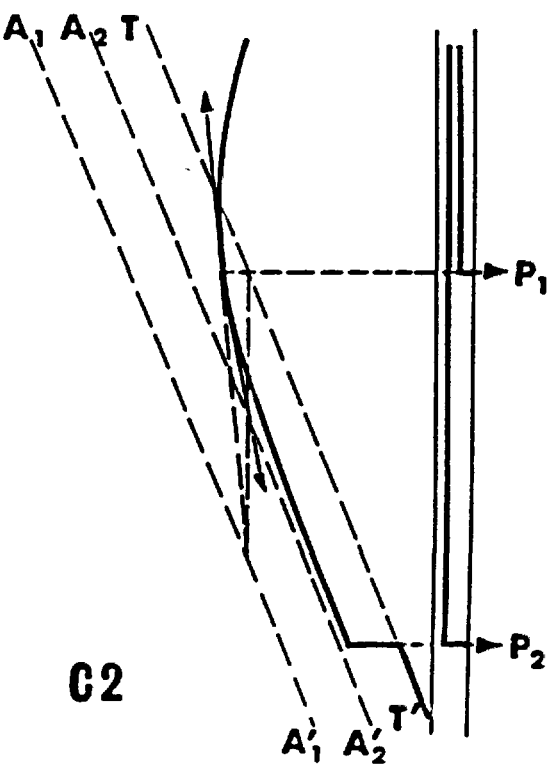

C2

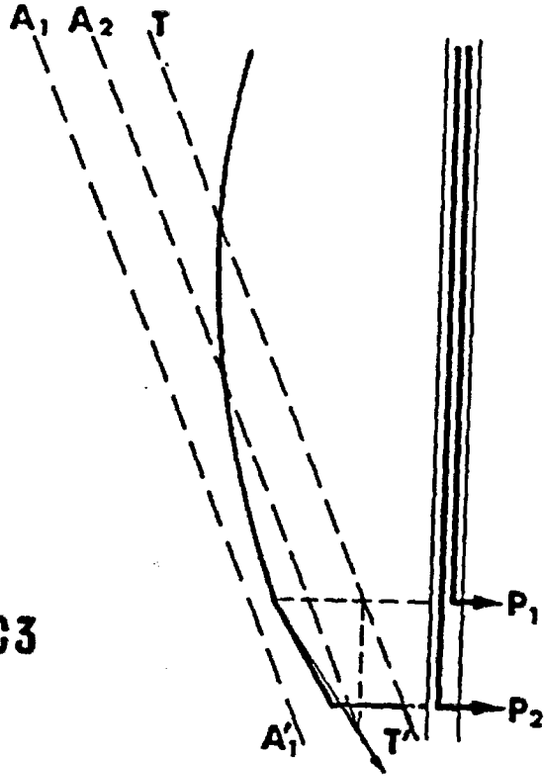
A1 A2 T
P1
P2
A'1
T'

C3

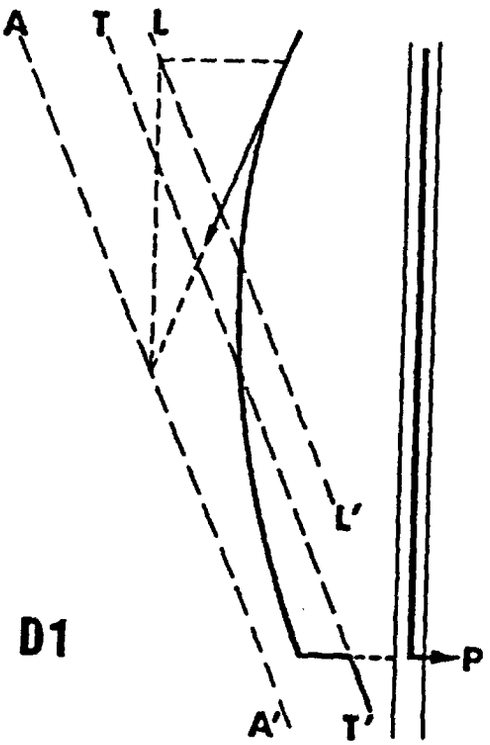
A T L
L'
P
A'
T'

D1

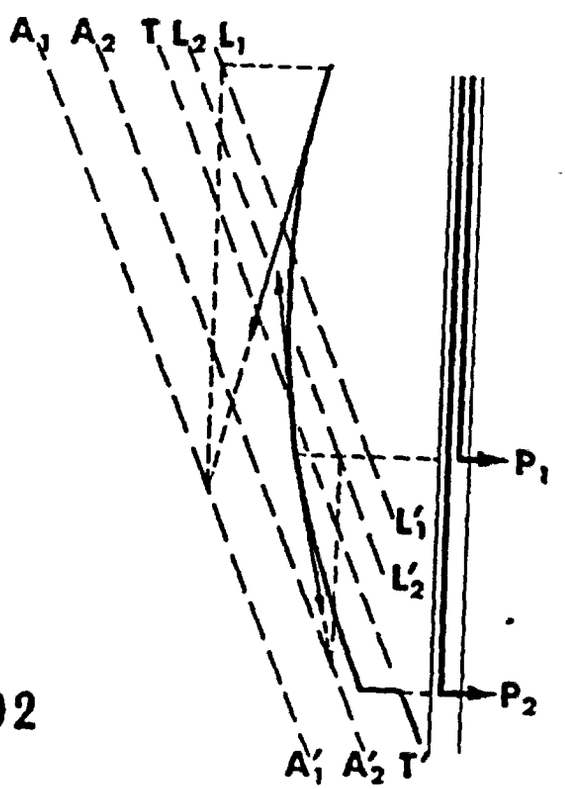
A1 A2 T L2 L1
P1
L'1
L'2
P2
A'1 A'2 T'

D2

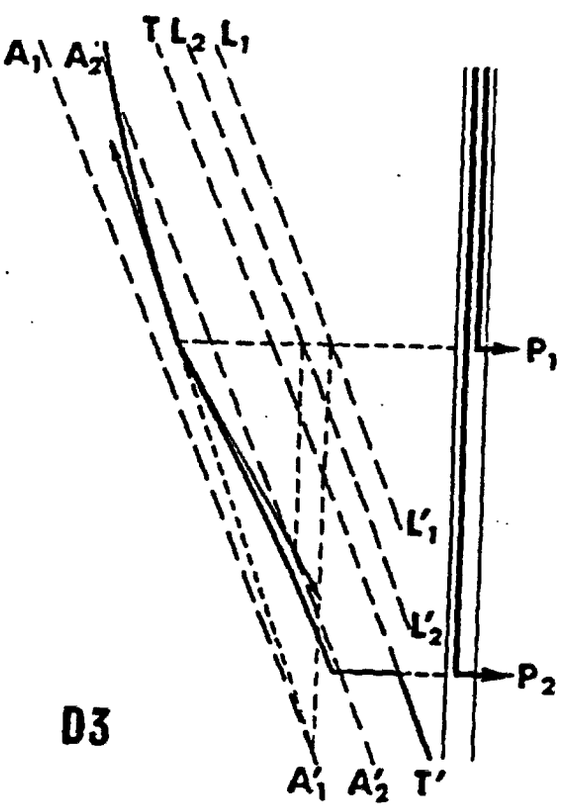
A1 A2 T L2 L1
P1
L'1
L'2
P2
A'1 A'2 T'

D3

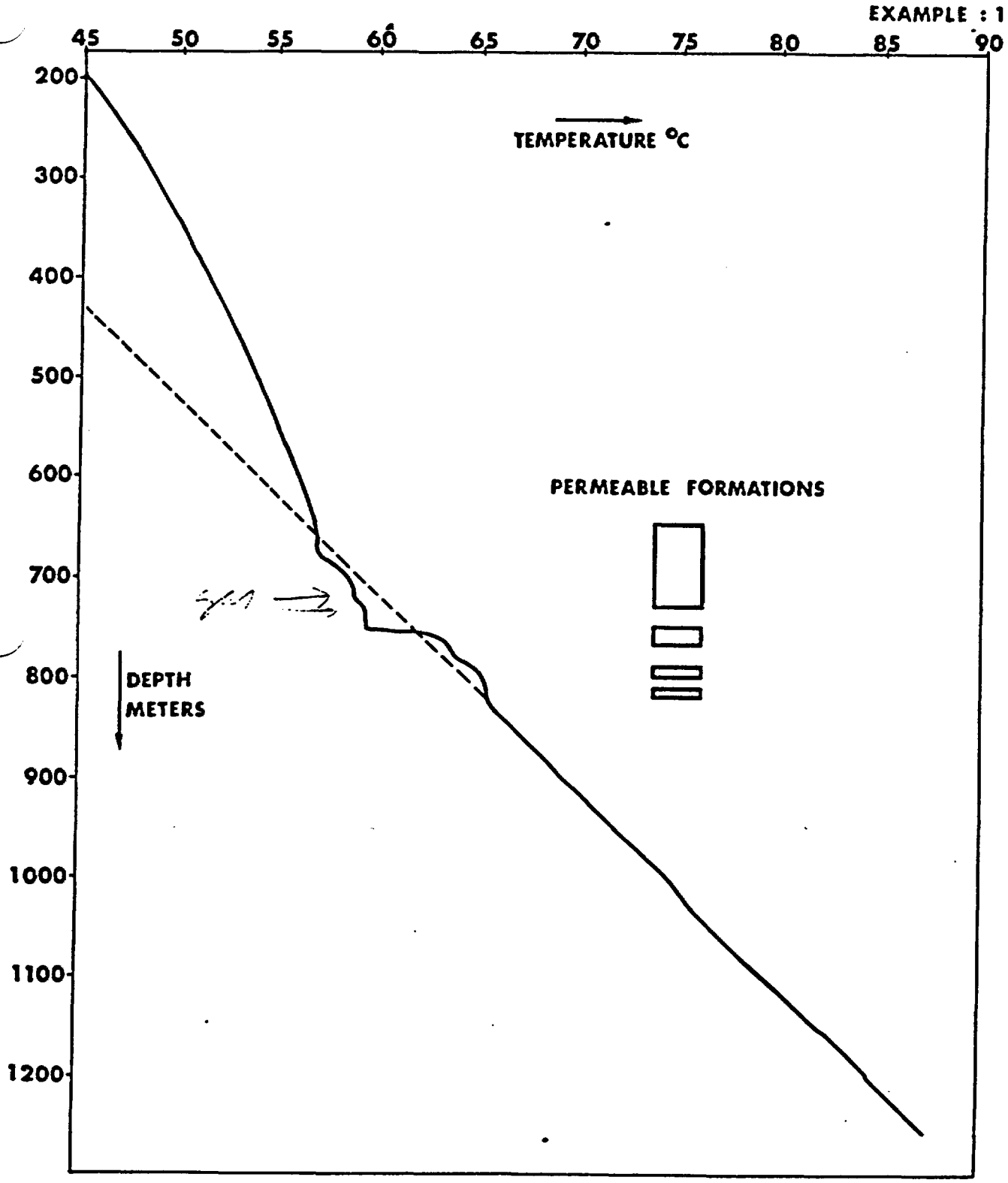
EXAMPLE : 1
45
50
55
60
65
70
75
80
85
90
200
300
400
500
600
700
800
900
1000
1100
1200
TEMPERATURE °C
PERMEABLE FORMATIONS
DEPTH
METERS

GRADIOMANOMETER

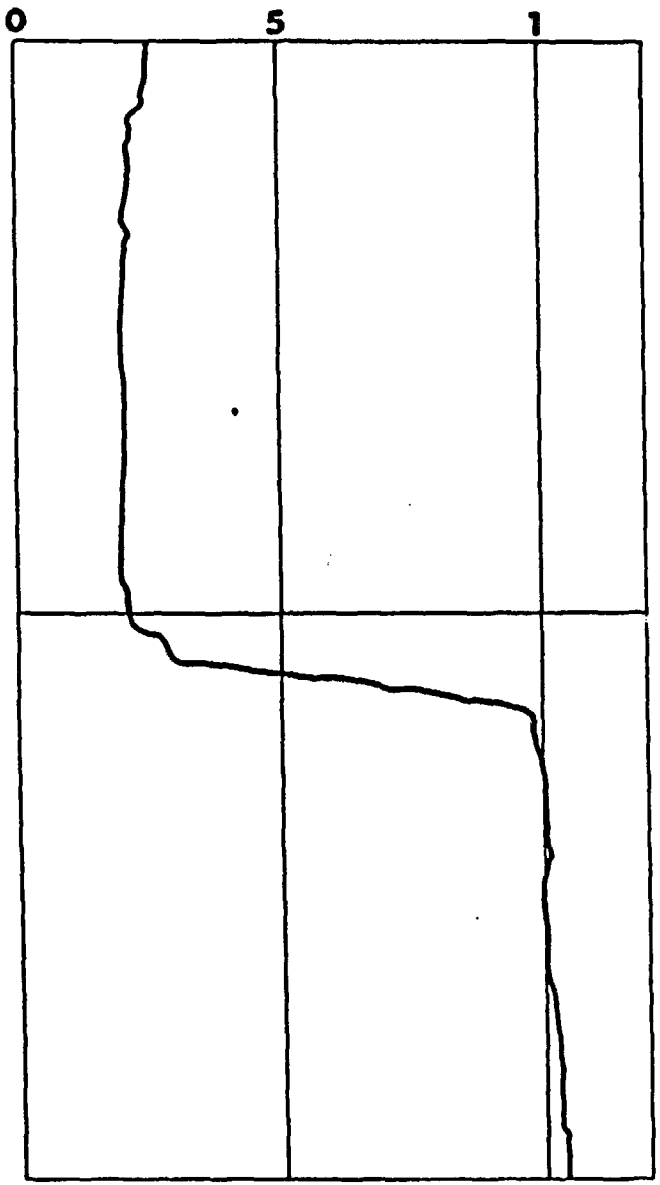

CONTINUOUS FLOWMETER (R.P.S)

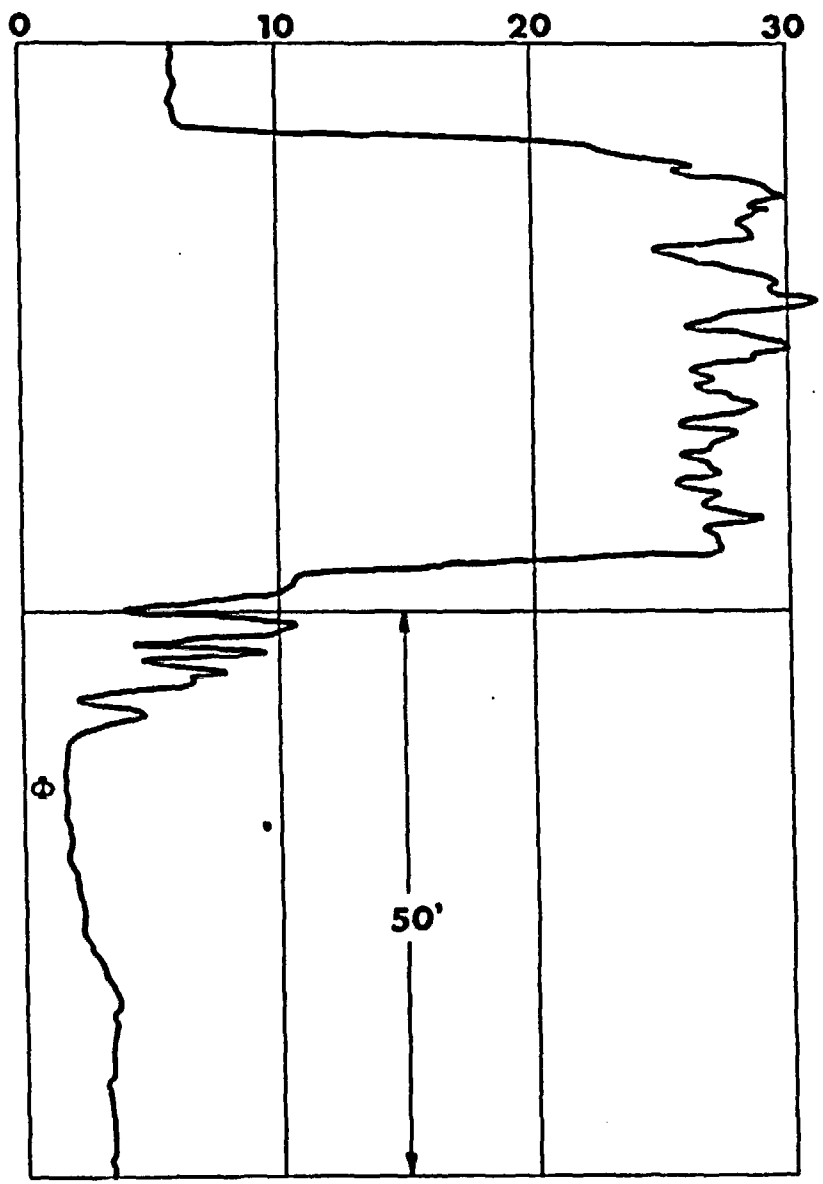

EXAMPLE : 2

7"CASING

$2\frac{1}{2}$" TUBING

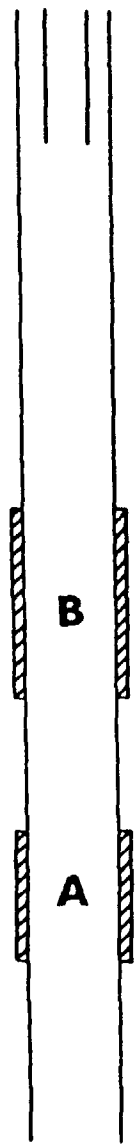

TEMPERATURE

EXAMPLE : 2

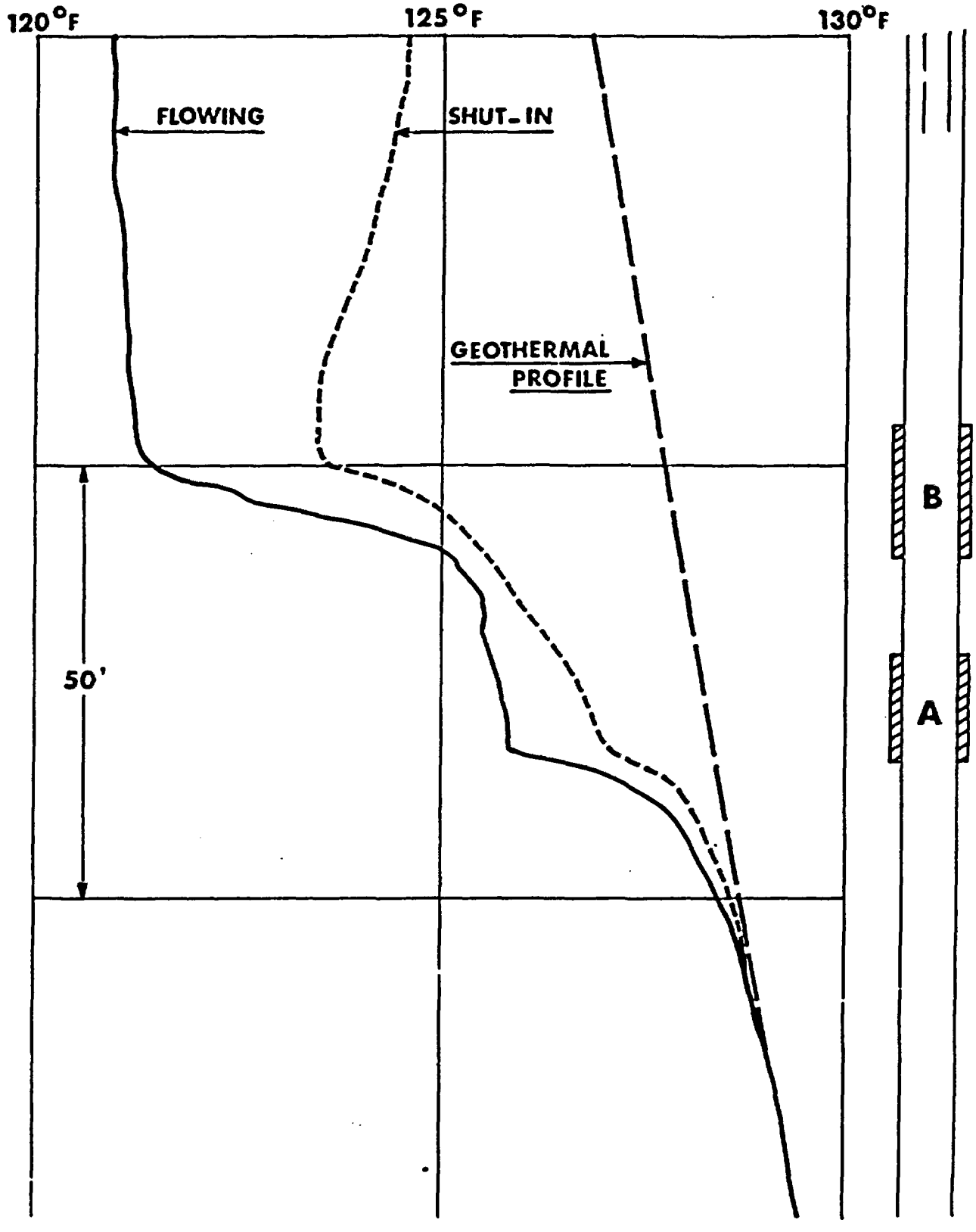

GRADIOMANOMETER

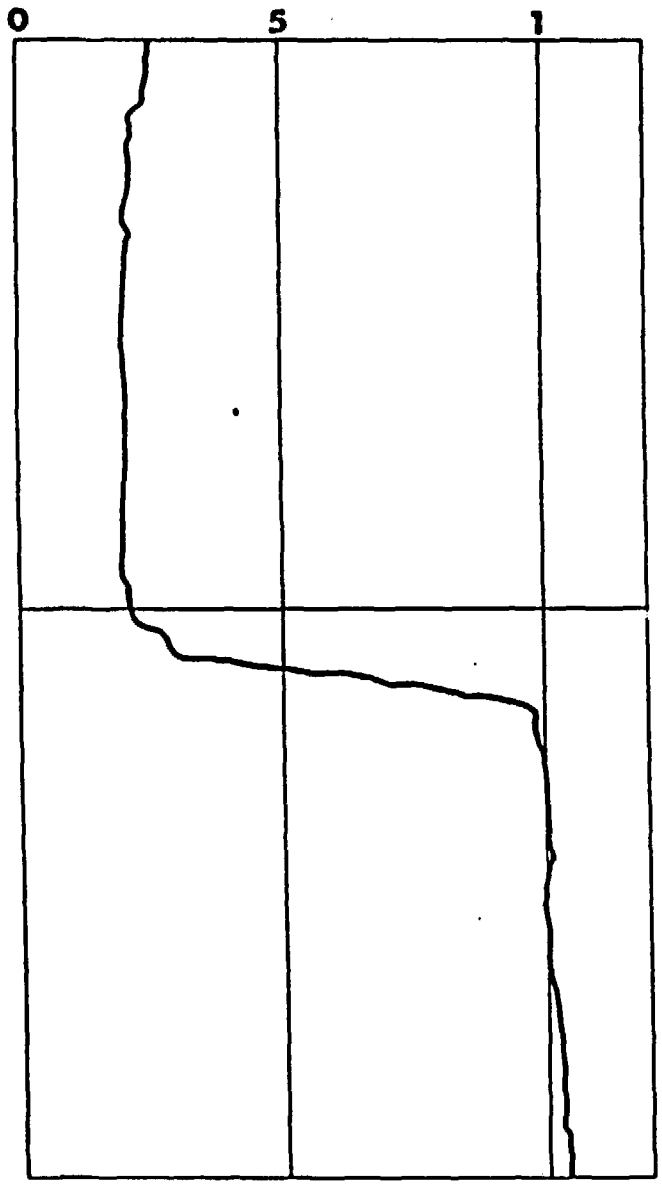

CONTINUOUS FLOWMETER (RPS)

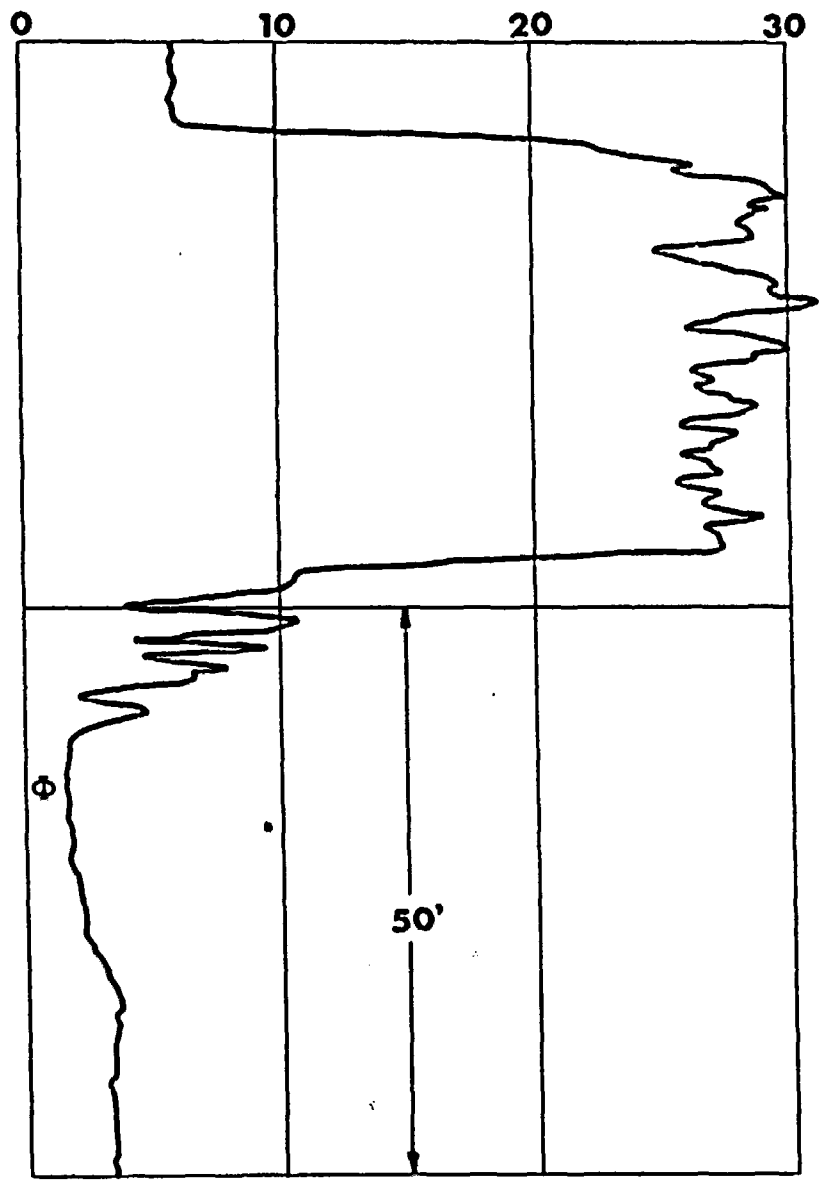

EXAMPLE : 2

7"CASING

$2\frac{1}{2}$" TUBING

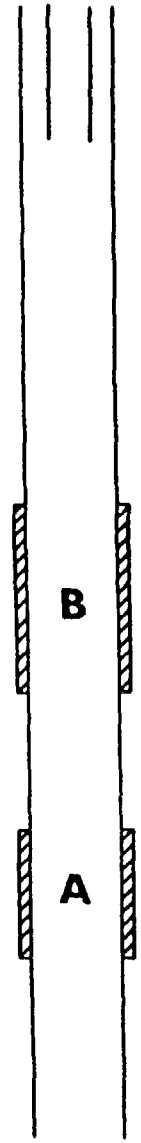

EXAMPLE: 4

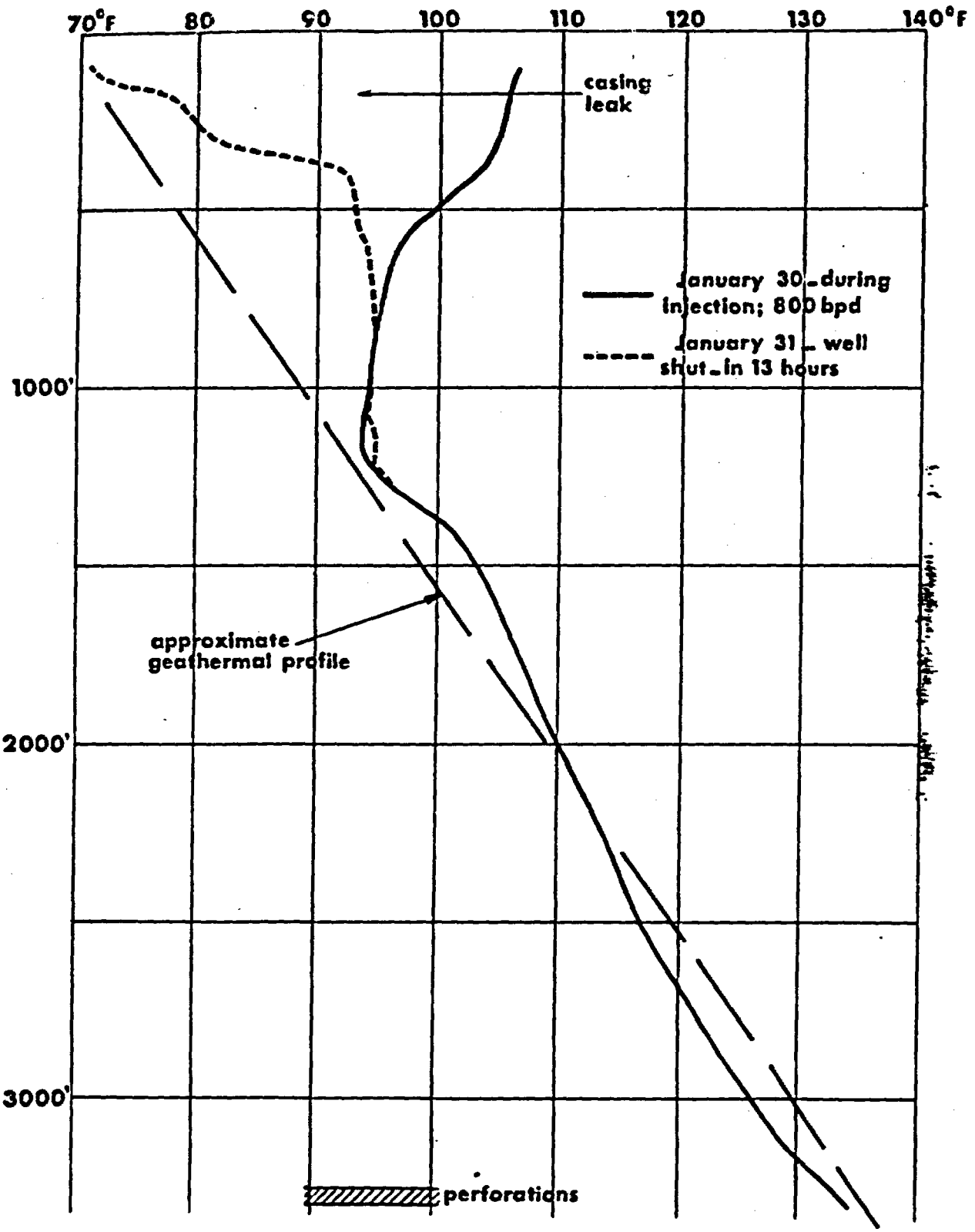
70°F
80
90
100
110
120
130
140°F
1000'
2000'
3000'
casing leak
January 30 - during injection; 800 bpd
January 31 - well shut-in 13 hours
approximate geothermal profile
perforations

Istavros S. PAPADOPULOS

NONSTEADY FLOW TO A WELL IN AN INFINITE ANISOTROPIC AQUIFER

SYMPOSIUM OF DUBROVNIK 1965

INTERNATIONAL ASSOCIATION OF SCIENTIFIC HYDROLOGY

NONSTEADY FLOW TO A WELL IN AN INFINITE ANISOTROPIC AQUIFER

Istavros S. PAPADOPULOS (1)
U.S. Geological Survey, Washington, D.C.

ABSTRACT

Well flow equations presently used in the analysis of pumping tests and the prediction of water levels have been derived under the assumption that aquifers are isotropic. These existing equations are not applicable to anisotropic aquifers such as fractured rocks.

In this paper, an equation is derived for the drawdown distribution around a well discharging at a constant rate from an infinite anisotropic aquifer. Drawdowns computed by this equation are compared and found to be in good agreement with those observed in an electric-analog model constructed for this purpose. It is shown that pumping test data from a minimum of three observation wells can be analyzed to obtain the components of the transmissibility tensor along an arbitrarily chosen set of axes, and that these components, in turn, can be used to determine the principal transmissibilities and the orientation of the principal axes. The method is illustrated with an example.

RÉSUMÉ

Écoulement irrégulier en direction d'un puits dans une nappe anisotrope illimitée

Les équations d'écoulement des puits actuellement utilisées pour l'analyse des tests de pompage et les prévisions des niveaux d'eau ont été établies sur le postulat que les aquifères sont isotropes. Ces équations ne peuvent être appliquées aux aquifères anisotropes que sont les roches fissurées.

L'auteur de cet article établit une équation donnant la répartition du rabattement de la nappe autour d'un puits au débit constant, foré dans une nappe anisotrope illimitée. Si l'on compare les rabattements calculés d'après cette équation à ceux que l'on observe sur un modèle électrique analogique construit à cette intention, on constate que les uns et les autres concordent. L'auteur montre aussi qu'en analysant les données des tests de pompage effectués sur un minimum de trois puits d'observation, on peut obtenir les composants du tenseur de transmissivité pour un ensemble d'axes arbitrairement choisis. Ces composants peuvent eux-mêmes être utilisés pour déterminer les transmissivités principales et l'orientation des axes principaux. La méthode est illustrée par un exemple.

INTRODUCTION

Equations presently used in analyses of pumping tests and predictions of water levels have been derived under the assumption that the aquifers are isotropic. These existing equations are not applicable to anisotropic aquifers such as some fractured rocks in which joint patterns cause variations of the permeability in different directions.

This paper derives an equation for the nonsteady drawdown distribution around a well discharging at a constant rate from an homogeneous anisotropic aquifer of infinite areal extent.

The flow of ground water in aquifers follows Darcy's law which states that the velocity is proportional to the negative gradient of the hydraulic head. In vectorial form this can be written as

$$\bar{V} = -K \operatorname{grad} h$$

where $\bar{V}$ is the velocity vector, the constant of proportionality K the permeability (hydraulic conductivity) of the aquifer, and h the hydraulic head.

(1) Present address: Dept. of Geol. and Geophys., Univ. of Minnesota, Minneapolis, Minn.

In anisotropic aquifers the velocity vector and the hydraulic gradient vector are generally not parallel. The constant of proportionality K is then a symmetric tensor of the second rank (Ferrandon, 1948; Scheidegger, 1954; Liakopoulos, 1962), usually referred to as the "permeability tensor", which transforms the components of the hydraulic gradient into those of the velocity. The velocity and the hydraulic gradient have the same direction only along one of three orthogonal axes called the "principal axes" of the permeability tensor. The anisotropy of an aquifer can be defined by the orientation of the principal axes and the magnitudes of the components of permeability along them.

For the two-dimensional flow problem treated in this paper use of the "transmissibility tensor" T, which is the product of the two-dimensional permeability tensor and the thickness of the aquifer, is convenient. In matrix notation the two-dimensional symmetric transmissibility tensor can be written as

$$T = \begin{vmatrix} T_{xx} & T_{xy} \\ T_{xy} & T_{yy} \end{vmatrix}$$

where x and y are an arbitrary set of orthogonal axes. For the principal axes ξ and η the above equation reduces to

$$T = \begin{vmatrix} T_{\xi\xi} & 0 \\ 0 & T_{\eta\eta} \end{vmatrix}$$

$T_{\xi\xi}$ and $T_{\eta\eta}$ being the maximum and minimum transmissibilities, respectively.

Analysis

The distribution of drawdown around a well of constant discharge which fully penetrates an infinite anisotropic artesian aquifer is described by the following boundary value problem

$$T_{xx}\frac{\partial^2 s}{\partial x^2} + 2T_{xy}\frac{\partial^2 s}{\partial x \partial y} + T_{yy}\frac{\partial^2 s}{\partial y^2} + Q\delta(x)\,\delta(y) = S\frac{\partial s}{\partial t} \qquad (1)$$

$$s(x, y, 0) = 0 \qquad (2)$$

$$s(\pm\infty, y, t) = 0 \qquad (3)$$

$$s(x, \pm\infty, t) = 0 \qquad (4)$$

where s is the drawdown, T_{xx}, T_{yy} and T_{xy} the components of the transmissibility tensor, S the storage coefficient, Q the discharge of the well, δ the Dirac delta function, x and y the coordinates of an arbitrary set of orthogonal axes with origin at the well, and t the time since the flow started.

The theory of integral transforms is used in solving the problem. By using the Laplace transformation with respect to t and initial condition 2 the problem can be expressed as

$$T_{xx}\frac{\partial^2 \bar{s}}{\partial x^2} + 2T_{xy}\frac{\partial^2 \bar{s}}{\partial x \partial y} + T_{yy}\frac{\partial^2 \bar{s}}{\partial y^2} + \frac{Q}{p}\delta(x)\,\delta(y) = Sp\bar{s} \qquad (5)$$

$$\bar{s}(\pm\infty, y, p) = 0 \qquad (6)$$

$$\bar{s}(x, \pm\infty, p) = 0 \qquad (7)$$

hydraulic gradient vector are
K is then a symmetric tensor
4; Liakopoulos, 1962), usually
forms the components of the
ity and the hydraulic gradient
onal axes called the "principal
aquifer can be defined by the
he components of permeability

this paper use of the "trans-
imensional permeability tensor
x notation the two-dimensional

For the principal axes ξ and η

missibilities, respectively.

tant discharge which fully
d by the following boundary

$$x)\,\delta(y) = S\frac{\partial s}{\partial t} \qquad (1)$$

(2)

(3)

(4)

onents of the transmissibility
ell, δ the Dirac delta function,
al axes with origin at the well,

ng the problem. By using the
ndition 2 the problem can be

$$x)\,\delta(y) = Sp\bar{s} \qquad (5)$$

(6)

(7)

where s is the Laplace transform of s, and p the parameter of the transformation Application of the complex Fourier transform with respect to x to the above equations results in

$$-T_{xx}\alpha^2 w - 2i\alpha T_{xy}\frac{\partial w}{\partial y} + T_{yy}\frac{\partial^2 w}{\partial y^2} + \frac{Q}{\sqrt{2\pi p}}\delta(y) = Spw \qquad (8)$$

$$w(\alpha, \pm\infty, p) = 0 \qquad (9)$$

where w is the transform of $\bar{s}$, α the parameter of the transformation and $i = \sqrt{-1}$. Transforming once more through use of the complex Fourier transform with respect to y yields an explicit expression for the transform of the solution

$$z = \frac{Q}{2\pi p}\,\frac{1}{T_{xx}\alpha^2 + 2T_{xy}\alpha\beta + T_{yy}\beta^2 + Sp} \qquad (10)$$

where z is the transform of w and β the parameter of the transformation.

Equation 10 is obtained irrespective of the order that the three transformations are made. Consequently, the order of inversion is irrelevant and can be chosen for convenience. Taking first the inverse Fourier transform with respect to y, one obtains

$$w = \frac{Q}{2\sqrt{2\pi}}\,\frac{\exp\{(iy\alpha T_{xy} - |y|[(T_{xx}T_{yy} - T_{xy}^2)\alpha^2 + ST_{yy}p]^{\frac{1}{2}})/T_{yy}\}}{p[(T_{xx}T_{yy} - T_{xy}^2)\alpha^2 + ST_{yy}p]^{\frac{1}{2}}} \qquad (11)$$

Then, taking the inverse Laplace transform through use of the convolution integral results in

$$L^{-1}\{w\} = \frac{Q\,e^{iy\alpha T_{xy}/T_{yy}}}{2\pi\sqrt{2ST_{yy}}}\int_0^t \exp\left[-\frac{y^2 S}{4T_{yy}\tau} - \frac{(T_{xx}T_{yy} - T_{xy}^2)\alpha^2\tau}{ST_{yy}}\right]\frac{d\tau}{\tau^{\frac{1}{2}}} \qquad (12)$$

where L^{-1} denotes the inverse Laplace transform of w. Finally, taking the inverse Fourier transform with respect to x, and after some mathematical manipulation we obtain the formal solution

$$s = \frac{Q}{4\pi\sqrt{T_{xx}T_{yy} - T_{xy}^2}}\,W(u_{xy}) \qquad (13)$$

where $W(u)$ is the negative exponential integral, known in the field of hydrology as the "well function", defined as

$$W(u) = \int_u^\infty \frac{e^{-\mu}}{\mu}\,d\mu$$

and in which

$$u_{xy} = \frac{S}{4t}\left(\frac{T_{xx}y^2 + T_{yy}x^2 - 2T_{xy}xy}{T_{xx}T_{yy} - T_{xy}^2}\right) \qquad (14)$$

If the coordinate axes x and y coincide with the principal axes ξ and η of the transmissibility tensor, equation 13 reduces to

$$s = \frac{Q}{4\pi\sqrt{T_{\xi\xi}T_{\eta\eta}}}\,W(u_{\xi\eta}) \qquad (15)$$

where $T_{\xi\xi}$ and $T_{\eta\eta}$ are the "principal transmissibilities" and

$$u_{\xi\eta} = \frac{S}{4t}\left(\frac{T_{\xi\xi}\eta^2 + T_{\eta\eta}\xi^2}{T_{\xi\xi}T_{\eta\eta}}\right) \tag{16}$$

Equation 15 is similar to one given by Collins [1961].

For small values of its argument, that is for $u < 0.02$, the well function appearing in equations 13 and 15 can be closely approximated [Cooper and Jacob, 1946] by

$$W(u) = -.5772 - \log_e u = 2.303 \log_{10} \frac{2.25}{4u}$$

Substituting this approximation in equations 13 and 15 one obtains solutions for relatively large values of time as

$$s = \frac{2.303\,Q}{4\pi\sqrt{T_{xx}T_{yy} - T_{xy}^2}} \log_{10}\left[\frac{2.25t}{S}\left(\frac{T_{xx}T_{yy} - T_{xy}^2}{T_{xx}y^2 + T_{yy}x^2 - 2T_{xy}xy}\right)\right] \tag{17}$$

for an arbitrary set of axes, and

$$s = \frac{2.303\,Q}{4\pi\sqrt{T_{\xi\xi}T_{\eta\eta}}} \log_{10}\left[\frac{2.25t}{S}\left(\frac{T_{\xi\xi}T_{\eta\eta}}{T_{\xi\xi}\eta^2 + T_{\eta\eta}\xi^2}\right)\right] \tag{18}$$

for the principal axes.

As an examination of the drawdown equations indicates, for a given time, lines of equal drawdown around a well pumping from an anisotropic aquifer have the form of concentric ellipses (fig. 1) with transverse axes along the maximum transmissibility axis ξ and conjugate axes along the minimum transmissibility axis η.

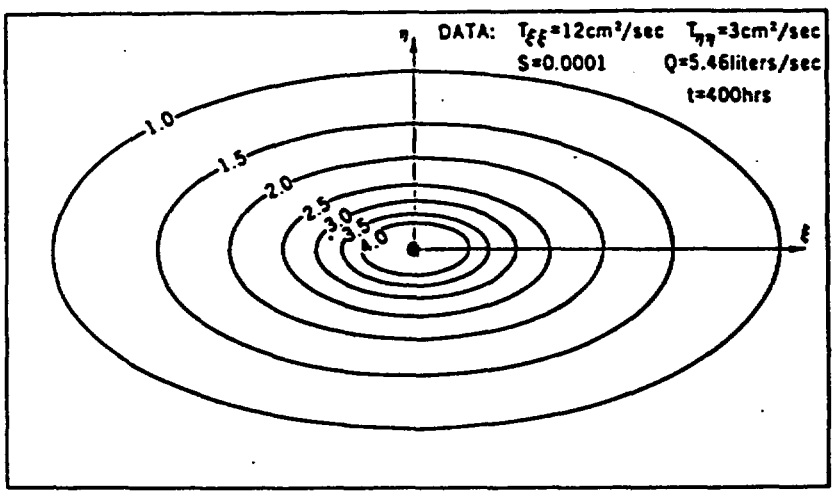

Fig. 1

ANALOG MODEL RESULTS

The analytical solutio
analog model consisting
was designed for an aquif
and 11 cm²/sec and a s
6.67 liters/sec. A node sp
One quadrant of the in
similate an infinite aqui
limits that would be reac

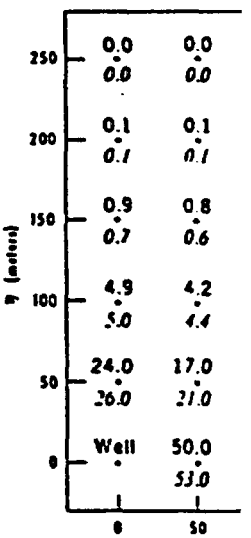

Measured and com
pumping, are shown on
with time at $\xi = 100$ n
representing the observe
screen. The measured a
differences being due to

APPLICATION TO PUMPI

The use of analytic
the transmissibility and
by some means. These
pumping tests, which co
equations for the flow

" and

(16)

2, the well function appearing
(Cooper and Jacob, 1946] by

$$3 \log_{10} \frac{2.25}{4u}$$

15 one obtains solutions for

$$\frac{-T_{xy}^2}{^2 - 2T_{xy}xy}\Big)\Big] \qquad (17)$$

$$\frac{T_{\xi\xi}T_{\eta\eta}}{l^2 + T_{\eta\eta}\xi^2}\Big)\Big] \qquad (18)$$

icates, for a given time, lines
sotropic aquifer have the form
e maximum transmissibility
ity axis η.

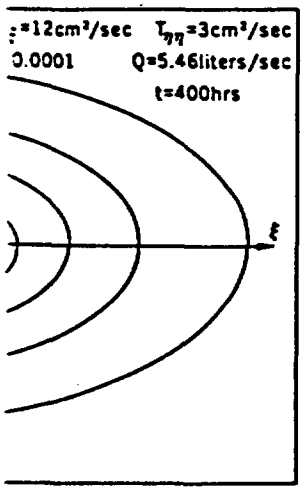

Analog model results

The analytical solution obtained in the previous pages was verified by an electric analog model consisting of a rectangular resistance-capacitance network. The model was designed for an aquifer having principal transmissibilities $T_{\xi\xi}$ and $T_{\eta\eta}$ of 37 cm²/sec. and 11 cm²/sec and a storage coefficient of 0.048. The well discharged at a rate of 6.67 liters/sec. A node spacing corresponding to a 50 meter orthogonal grid was chosen. One quadrant of the infinite space bounded by the ξ and η axes was modeled. To similate an infinite aquifer the model was extended in both directions beyond the limits that would be reached by the effect of pumping within the period of measurement.

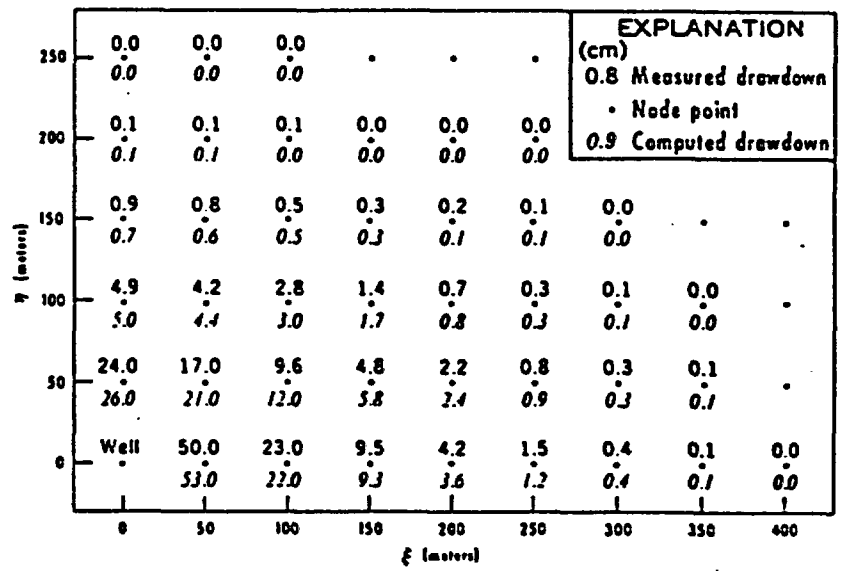

Fig. 2

Measured and computed drawdowns at each node point, for 10^5 seconds of pumping, are shown on figure 2. Variation of the computed and observed drawdown with time at $\xi = 100$ meters and $\eta = 100$ meters is shown on figure 3. The curve representing the observed drawdown was traced from a photograph of the oscilloscope screen. The measured and computed values in the two figures agree closely, the slight differences being due to instrumental error.

Application to pumping tests

The use of analytical solutions in quantitative hydrologic studies requires that the transmissibility and storage coefficient of the aquifers be determined or estimated by some means. These formation constants are usually determined from analyses of pumping tests, which consist of relating observed drawdowns to theoretical drawdown equations for the flow system under consideration. For anisotropic aquifers the

appropriate theoretical equations are equations 13 or 17 if the principal axes are not known, and equations 15 or 18 if the principal axes are known. The method of analysis is essentially the "type-curve" or, if applicable, the "straight-line" method, both of which are well known to hydrologists from their use in the analyses of tests of isotropic aquifers. The observed drawdown s is plotted against time t or reciprocal of time $1/t$ for each observation well. Because of the absence of radial symmetry, the composite drawdown graph (s against r^2/t, where r is the radial distance) and the distance-drawdown (s against r) plots which are used in tests of isotropic aquifers,

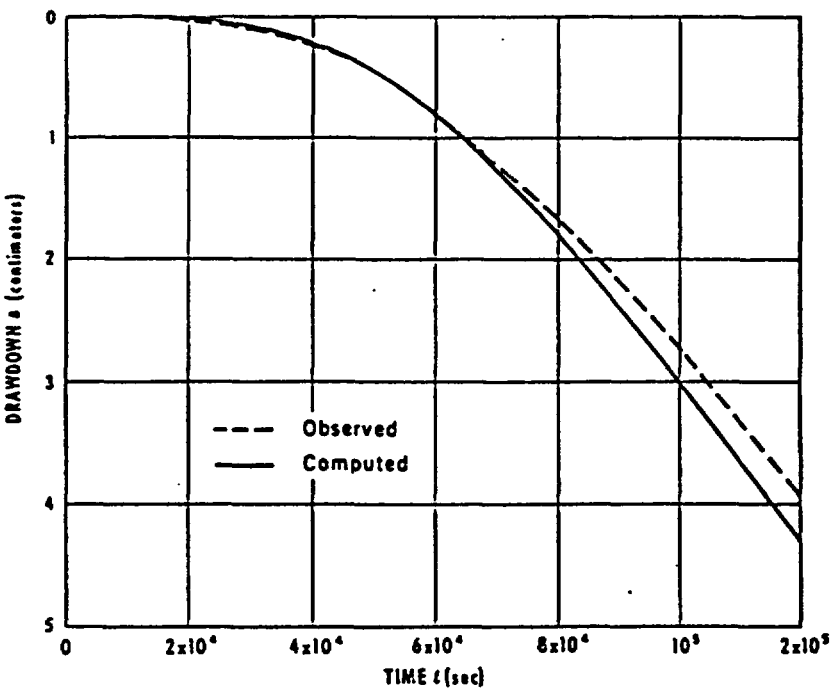

Fig. 3

cannot be used in tests of anisotropic aquifers. Also, since there are four constants to be determined (the three transmissibility components T_{xx}, T_{yy} and T_{xy} and the storage coefficient S) a minimum of three observation wells at different distances and different directions from the pumping well are necessary.

Both the type-curve and the straight-line methods of analysis for anisotropic aquifers are outlined below for the case where only three observation wells exist and the directions of the principal axes are not known. When data from more than three observation wells are available the same approach can be used by grouping them into sets of three.

Type-curve method

1. Choose a convenient rectangular coordinate system with the origin at the pumping well and record the x and y coordinates of each observation well.

if the principal axes are not
own. The method of analysis
raight-line" method, both of
in the analyses of tests of
against time t or reciprocal
sence of radial symmetry, the
the radial distance) and the
in tests of isotropic aquifers,

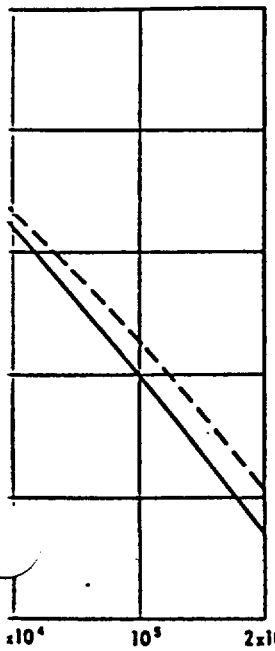

ce there are four constants to
, T_{yy} and T_{xy} and the storage
fferent distances and different

s of analysis for anisotropic
e observation wells exist and
n data from more than three
e used by grouping them into

stem with the origin at the
ch observation well.

2. From tables of the well function $W(u)$ [Wenzel, 1942] prepare a type curve of $W(u_{xy})$ against u_{xy} on logarithmic paper. The curve so obtained is known as the type curve.

3. Plot observed values of the drawdown s against reciprocal time $1/t$ for each of the three observation wells on logarithmic paper to the same scale as the type curve.

4. Superpose the observed data plot on the type curve and, keeping the coordinate axes of the two plots parallel, find, for each well, the best fit of the data on the type curve. Choose a match point for each well and record the dual coordinates $W(u_{xy})$, s, u_{xy} and $1/t$ of each match point.

5. Substitute the values of $W(u_{xy})$ and s from each match point into equation 13 and solve for $(T_{xx}T_{yy}-T_x^2{}_y)$. All three match points should yield the same, or approximately the same, value for $(T_{xx}T_{yy}-T_x^2{}_y)$. If they do not, judgement must be used to obtain an "average" value.

6. Substitute the values of u_{xy} and $1/t$ from each match point and the value of $(T_{xx}T_{yy}-T_x^2{}_y)$ obtained in step 5 into equation 14 and, using the coordinates of the observation well corresponding to each match point, solve the resulting three equations for the products ST_{xx}, ST_{yy} and ST_{xy}.

7. Solve these products for T_{xx}, T_{yy} and T_{xy} in terms of S and, substituting these into the expression $(T_{xx}T_{yy}-T_x^2{}_y)$ whose value is known from step 5, obtain S.

8. Having found S, calculate T_{xx}, T_{yy} and T_{xy} from the products obtained in step 6.

Sraight-line method

The straight-line method of analysis can be used only if all or the latter part of the observed drawdown data for all three observation wells falls within the range of time for which equation 17 is applicable.

1. Same as step 1 of type-curve method.

2. Plot observed values of drawdown s in each observation well against time t on semilogarithmic paper with t on the logarithmic scale. If the latter data plot as a straight line equation 17 probably applies.

3. For each well draw a straight line through those points that plot as a straight line. An examination of equation 17 shows that this straight line has a slope (Δs per log cycle) given by

$$\frac{\Delta s}{\text{cycle}} = \frac{2.303\,Q}{4\pi\sqrt{T_{xx}T_{yy}-T_{xy}^2}} \tag{19}$$

and a t-intercept t_0 given by

$$t_0 = \frac{S}{2.25}\left(\frac{T_{xx}y^2+T_{yy}x^2-2T_{xy}xy}{T_{xx}T_{yy}-T_{xy}^2}\right) \tag{20}$$

4. Find the intercept t_0 and the slope Δs/cycle of each line. All three lines should have the same, or approximately the same, slope. If differences exist obtain an average value.

5. Substitute the slope in equation 19 and calculate $(T_{xx}T_{yy}-T_x^2{}_y)$.

6. Substitute the intercept t_0 of each line and the value of $(T_{xx}T_y^2{}_y-T_{xy})$ obtained in step 5 into equation 20 and, using the coordinates of the observation well corresponding to each intercept, solve the resulting three equations for the products ST_{xx}, ST_{yy} and ST_{xy}.

7. Follow the same procedure as in steps 7 and 8 of the type curve method to calculate S, T_{xx}, T_{yy} and T_{xy}.

After the components T_{xx}, T_{yy} and T_{xy} of the transmissibility tensor are obtained from the type-curve or the straight-line method, the principal transmissibilities $T_{\xi\xi}$ and $T_{\eta\eta}$ and the orientation of the principal axes can be determined by making use of tensor properties. The following relations, obtained from the invariants and the rules of transformation of tensors, apply for all symmetric tensors of the second rank:

$$T_{\xi\xi} = \tfrac{1}{2}\{(T_{xx}+T_{yy}) + [(T_{xx}-T_{yy})^2 + 4T_{xy}^2]^{\frac{1}{2}}\} \tag{21}$$

$$T_{\eta\eta} = \tfrac{1}{2}\{(T_{xx}+T_{yy}) - [(T_{xx}-T_{yy})^2 + 4T_{xy}^2]^{\frac{1}{2}}\} \tag{22}$$

$$\theta = \arctan\left(\frac{T_{\xi\xi}-T_{xx}}{T_{xy}}\right) \tag{23}$$

where θ is the angle between the x and the ξ axis, positive in a counterclockwise direction from the x-axis, and restricted for convenience to the interval $0 \leq \theta < \pi$.

Illustrative example

A 12-hour pumping test was conducted to determine the hydraulic properties of an anisotropic aquifer. The well PW was pumped at a rate of 12.57 liters/sec. and the drawdown was observed at three observation wells OW-1, OW-2 and OW-3 located as shown on figure 4. The drawdown data are given on table 1. The problem is to find the storage coefficient and principal transmissibilities of the aquifer and the direction of the principal axes.

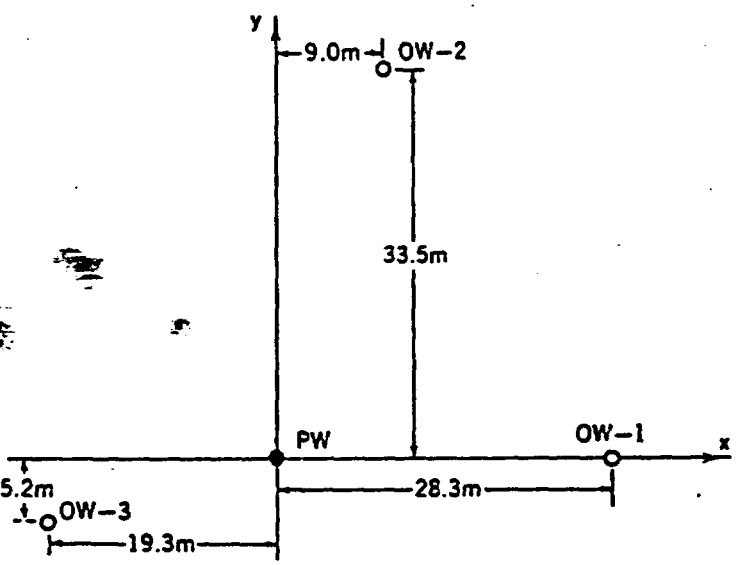

Fig. 4

Solution

The coordinate a
coordinates of the o

OW
OW
OW

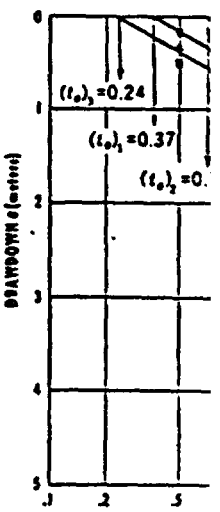

A semilogarithmic p
analysis is applicable.
is the same for all t
t-intercepts are:

From equation 19 w

$$(T_{xx}T_{yy} - T_{xy}^2) = \left[$$

sibility tensor are obtained
cipal transmissibilities $T_{\xi\xi}$
determined by making use
the invariants and the rules
ors of the second rank:

$$+ 4T_{xy}^2]^{\frac{1}{2}}\} \quad (21)$$

$$+ 4T_{xy}^2]^{\frac{1}{2}}\} \quad (22)$$

$$(23)$$

tive in a counterclockwise
to the interval $0 \leqslant \theta < \pi$.

the hydraulic properties of
of 12.57 liters/sec. and the
, *OW*-2 and *OW*-3 located
table 1. The problem is to
es of the aquifer and the

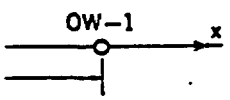

Solution

The coordinate axes are chosen with the x-axis passing through *OW*-1 and the coordinates of the observation wells are determined as

$$\left.\begin{aligned} OW/1\text{-}\ x &= 28.3\ \text{m};\ y = 0 \\ OW/2\text{-}\ x &= 9.0\ \text{m};\ y = 33.5\ \text{m} \\ OW/3\text{-}\ x &= -19.3\ \text{m};\ y = -5.2\ \text{m} \end{aligned}\right\} \quad (24)$$

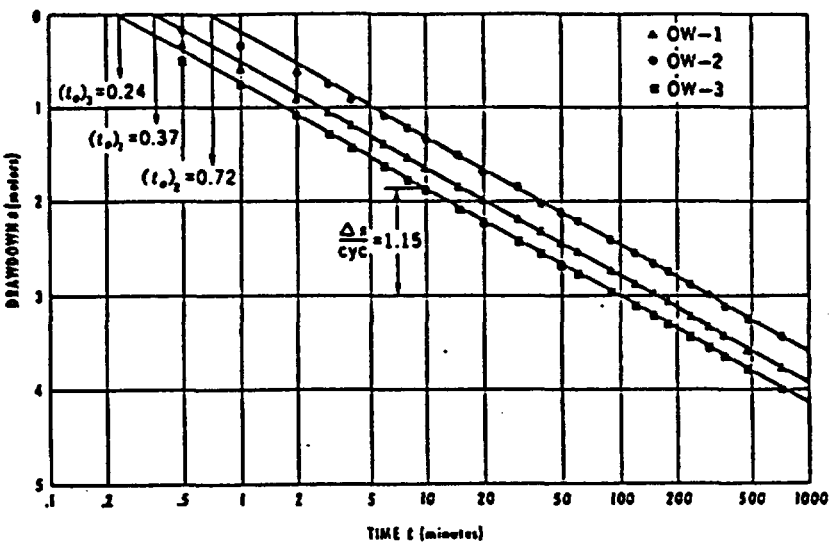

Fig. 5

A semilogarithmic plot of the data (fig. 5) shows that the straightline method of analysis is applicable. The slope of the lines drawn through the latter part of the data is the same for all three lines and has the value of 1.15 meters per log cycle. The t-intercepts are:

$$\left.\begin{aligned} (t_0)_1 &= 0.37\ \text{min.} \\ (t_0)_2 &= 0.72\ \text{min.} \\ (t_0)_3 &= 0.24\ \text{min.} \end{aligned}\right\} \quad (25)$$

From equation 19 we obtain

$$(T_{xx}T_{yy} - T_{xy}^2) = \left[\frac{2.303 \times 12.57\ \text{liters/sec.}}{4\pi \times 1.15\ \text{m} \times 1000\ \text{liter/m}^3}\right]^2 = 4 \times 10^{-6}\ \text{m}^4/\text{sec}^2. \quad (26)$$

Substituting from (24), (25) and (26) into equation 20 we find

$$(28.3)^2\, ST_{yy} = 2.00 \times 10^{-4}\ \text{m}^4/\text{sec.}$$

$$(33.5)^2\, ST_{xx} + (9.0)^2\, ST_{yy} - 2(33.5)\,(9.0)\, ST_{xy} = 3.89 \times 10^{-4}\ \text{m}^4/\text{sec.}$$

$$(5.2)^2\, ST_{xx} + (19.3)^2\, ST_{yy} - 2(5.2)\,(19.3)\, ST_{xy} = 1.39 \times 10^{-4}\ \text{m}^4/\text{sec.}$$

Solving these three equations simultaneously we obtain

$$\left.\begin{aligned} T_{xx} &= \frac{2.5 \times 10^{-7}}{S}\ \text{m}^2/\text{sec.} \\ T_{yy} &= \frac{2.5 \times 10^{-7}}{S}\ \text{m}^2/\text{sec.} \\ T_{xy} &= -\frac{1.5 \times 10^{-7}}{S}\ \text{m}^2/\text{sec.} \end{aligned}\right\} \qquad (27)$$

Substituting from (27) into (26) gives

$$\frac{6.25 \times 10^{-14} - 2.25 \times 10^{-14}}{S^2} = 4 \times 10^{-6}$$

or

$$S = 10^{-4} \qquad (28)$$

Finally, by substituting from (28) into (27) we have

$$T_{xx} = 2.5 \times 10^{-3}\ \text{m}^2/\text{sec.} = 25\ \text{cm}^2/\text{sec.}$$

$$T_{yy} = 2.5 \times 10^{-3}\ \text{m}^2/\text{sec.} = 25\ \text{cm}^2/\text{sec.}$$

$$T_{xy} = -1.5 \times 10^{-3}\ \text{m}^2/\text{sec.} = -15\ \text{cm}^2/\text{sec.}$$

With the components of the transmissibility tensor now known, the principal transmissibilities are obtained from equation 21 and 22 as

$$T_{\xi\xi} = \tfrac{1}{2}\{(25+25) + [4 \times (-15)^2]^{\frac{1}{2}}\} = 40\ \text{cm}^2/\text{sec.}$$

$$T_{\eta\eta} = \tfrac{1}{2}\{(25+25) - [4 \times (-15)^2]^{\frac{1}{2}}\} = 10\ \text{cm}^2/\text{sec.}$$

The angle θ between x and ξ axis is found from equation 23 to be

$$\theta = \arctan\left[\frac{40-25}{-15}\right]$$

$$= \arctan(-1)$$

$$= 135^\circ$$

Drawdown

Time t since pun started minut
0.5
1
2
3
4
6
8
10
15
20
30
40
50
60
90
120
150
180
240
300
360
480
720

COLLINS, R.E. 1961
Publishing Corp.
COOPER, H.H. Jr. an
formation consta
vol. 27, no. IV, p
FERRANDON, J. 1948
pp. 24-28.
LIAKOPOULOS, A. 19
Engineering, Am
SCHEIDEGGER, A.E.
fluids. *Geofisic*
WENZEL, L.K. 1942
192 p. (U.S. Geo

sec.

3.89×10^{-4} m^4/sec.

1.39×10^{-4} m^4/sec.

(27)

10^{-6}

(28)

/sec.

/sec.

now known, the principal
as

= 40 cm^2/sec.

= 10 cm^2/sec.

n 23 to be

TABLE 1

Drawdown data from observations well OW-1, OW-2, and OW-3

Time t since pumping started minutes)	Drawdown s (meters) OW-1	OW-2	OW-3
0.5	0.335	0.153	0.492
1	0.591	0.343	0.762
2	0.911	0.611	1.089
3	1.082	0.762	1.284
4	1.215	0.911	1.419
6	1.405	1.089	1.609
8	1.549	1.225	1.757
10	1.653	1.329	1.853
15	1.853	1.531	2.071
20	2.019	1.677	2.210
30	2.203	1.853	2.416
40	2.344	2.019	2.555
50	2.450	2.123	2.670
60	2.541	2.210	2.750
90	2.750	2.416	2.963
120	2.901	2.555	3.118
150	2.998	2.670	3.218
180	3.075	2.750	3.310
240	3.235	2.901	3.455
300	3.351	2.998	3.565
360	3.438	3.118	3.649
480	3.587	3.247	3.802
720	3.784	3.455	3.996

REFERENCES

COLLINS, R.E. 1961. *Flow of fluids through porous materials.* New York, Reinhold Publishing Corp. p. 115.

COOPER, H.H. Jr. and JACOB, C.E. 1946. A generalized graphical method for evaluating formation constants and summarizing wellfield history. *Trans. Am. Geophys. Union*, vol. 27, no. IV, pp. 526-534.

FERRANDON, J. 1948. Les lois de l'écoulement de filtration. *Génie civil*, vol. 125, no. 2, pp. 24-28.

LIAKOPOULOS, A. 1962. On the tensor concept of the hydraulic conductivity. *Review of Engineering*, Am. Univ. of Beirut, no. 4, pp. 35-42.

SCHEIDEGGER, A.E. 1954. Directional permeability of porous media to homogeneous fluids. *Geofisica Pura e Applicata*, vol. 28, pp. 75-90.

WENZEL, L.K. 1942. *Methods of determining permeability of waterbearing materials*, 192 p. (U.S. Geol. Survey Water-Supply Paper 887.)